Supplemental Table 1. Data Used for Trio Analysis.

Sample	HiFi Coverage	ONT Coverage	CLR Coverage
HG002	35.2499	46.6151	54.8693
HG003	33.6795	80.6551	25.6278
HG004	33.1812	83.1599	23.4694

Source: https://ftp-trace.ncbi.nlm.nih.gov/ReferenceSamples/giab/data/AshkenazimTrio/

Supplemental Table 2. Data Used for Cohort Analysis.

Tech	Sample	Coverage	Study	Ancestry
HiFi	HG001	29.4987	GIAB	CEU
HiFi	HG00512	29.3707	1KGP	CHS
HiFi	HG00513	40.3823	1KGP	CHS
HiFi	HG006	32.4010	GIAB	CHS
HiFi	HG00731	32.9366	1KGP	PUR
HiFi	HG00732	21.2571	1KGP	PUR
HiFi	HG007	36.1509	GIAB	CHS
HiFi	HG01109	31.7902	HPRC+	PUR
HiFi	HG01243	34.8145	HPRC+	PUR
HiFi	HG01442	36.9866	HPRC+	CLM
HiFi	HG02055	39.0903	HPRC+	ACB
HiFi	HG02080	33.7257	HPRC+	KHV
HiFi	HG02109	30.2620	HPRC+	ACB
HiFi	HG02145	35.7587	HPRC+	ACB
HiFi	HG02723	45.4921	HPRC+	GWD
HiFi	HG03098	35.1080	HPRC+	MSL
HiFi	HG03492	33.2615	HPRC+	PJL
HiFi	NA19238	24.9931	1KGP	YRI
HiFi	NA19239	25.8028	1KGP	YRI
ONT	HG003	80.6551	GIAB	ASH
ONT	HG004	83.1599	GIAB	ASH
CLR	AK1	79.2865	Audano	EAS
CLR	CHM13	97.1029	Audano	EUR*
CLR	CHM1	51.2768	Audano	EUR*
CLR	HG00268	69.5876	Audano	FIN
CLR	HG01352	56.2097	Audano	CLM
CLR	HG02059	63.9237	Audano	KHV
CLR	HG02106	59.9712	Audano	PEL
CLR	HG04217	128.5960	Audano	ITU
CLR	HX1	76.6489	Audano	EAS
CLR	NA19434	58.3505	Audano	LWK

*Hydatidiform mole for which only the super-population has been reported

1KGP: http://ftp.1000genomes.ebi.ac.uk/vol1/ftp/data_collections/HGSVC2/working/
GIAB: http://ftp-trace.ncbi.nlm.nih.gov/giab/ftp/data
HPRC+: https://github.com/human-pangenomics/HPP_Year1_Data_Freeze_v1.0
Audano: [22]

Supplemental Table 3. Software Versions.

Software	Version
Jasmine	1.1.0
Iris	1.0.4
sniffles	1.0.11
winnowmap	2.0
racon	1.4.10
minimap2	2.17
samtools	1.9
SURVIVOR	1.0.7
svtools	0.5.1
svimmer	0.1
dbsvmerge	commit 85b3687a54ce21ba25862c58707daa212b9fbcbd
svpop	commit 8be50c55f8e81f8c701077bb9c00ee5bea3e0d2b
sv-merger	commit b7745239348c7a6623efa516bd2841b53ff6046a
Paragraph	2.4
CAVIAR	commit 135b58baffac92b5e9b45f8db78315a9b4d713bc
plink	1.90b6.4
snphwe	1.0.2

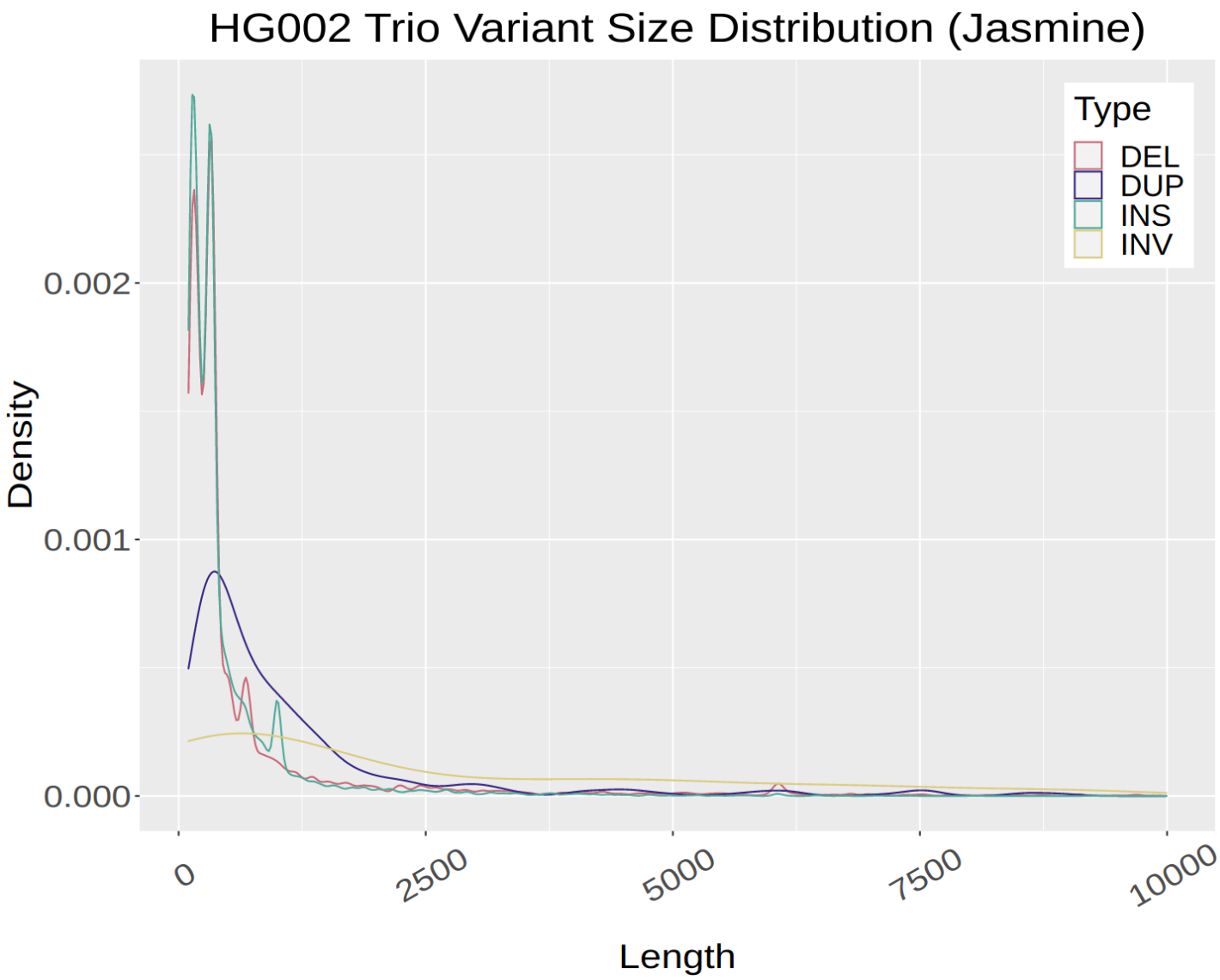

Supplementary Figure 1. HG002 Trio HiFi Variant Size Density
The density distribution of variant sizes called in the HG002 trio from HiFi data. The spikes in the distribution around 300bp and 6-7kbp correspond to SINE and LINE elements, respectively.

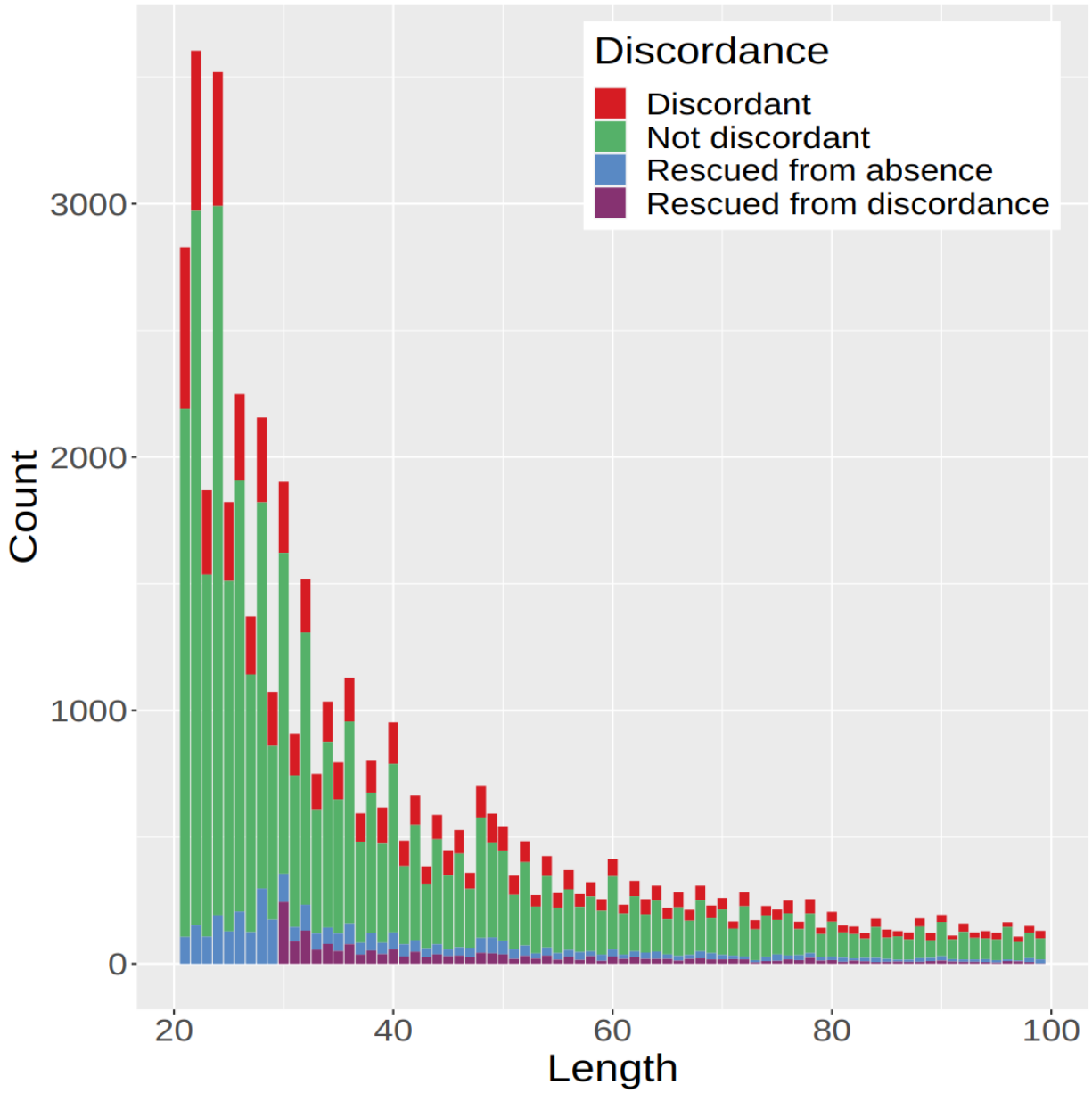

Supplementary Figure 2. Discordance by Length with Double Thresholding.
The benefits of using “double thresholding” to improve variant discovery in HG002 while also reducing the rate of Mendelian discordance. SVs and indels were called with a more lenient length threshold of 20bp, but only those which were merged with a variant with length at least 30bp in a different sample were kept. “Rescued from absence” refers to variants which would have been missed in HG002 using a single threshold. “Rescued from discordance” refers to variants which would have been discordant in HG002 with a single threshold, but which we were able to detect in one or both parents with double thresholding.

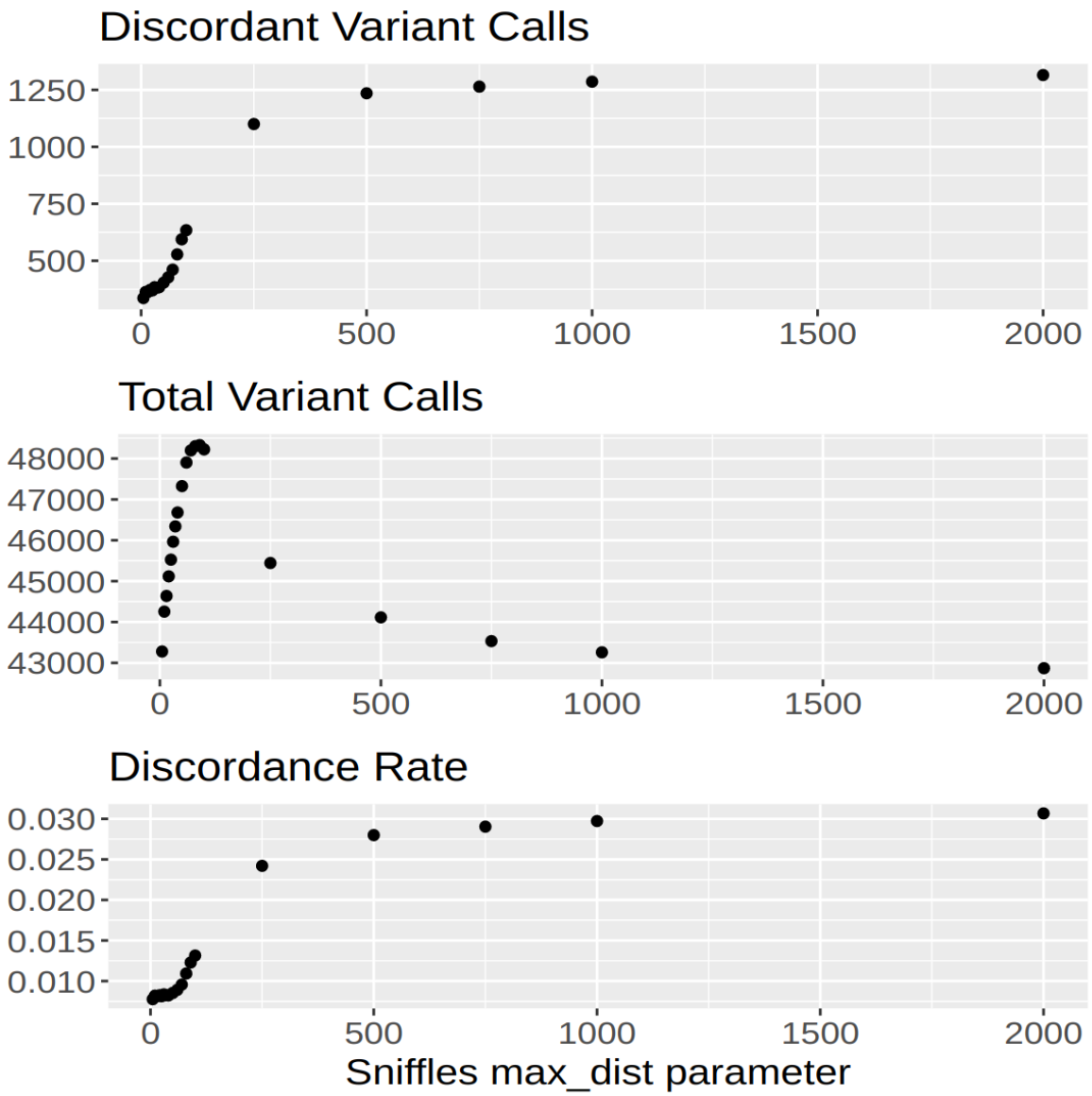

Supplementary Figure 3. Optimized Variant Calling Parameters for HiFi.
We called SVs and indels in HG002, HG003, and HG004 from HiFi reads using different values of the *max_dist* parameter in sniffles and merged each trio callset with Jasmine. For each *max_dist* value we measured the total number of variants in the trio, the number of discordant variants, and the discordance rate.

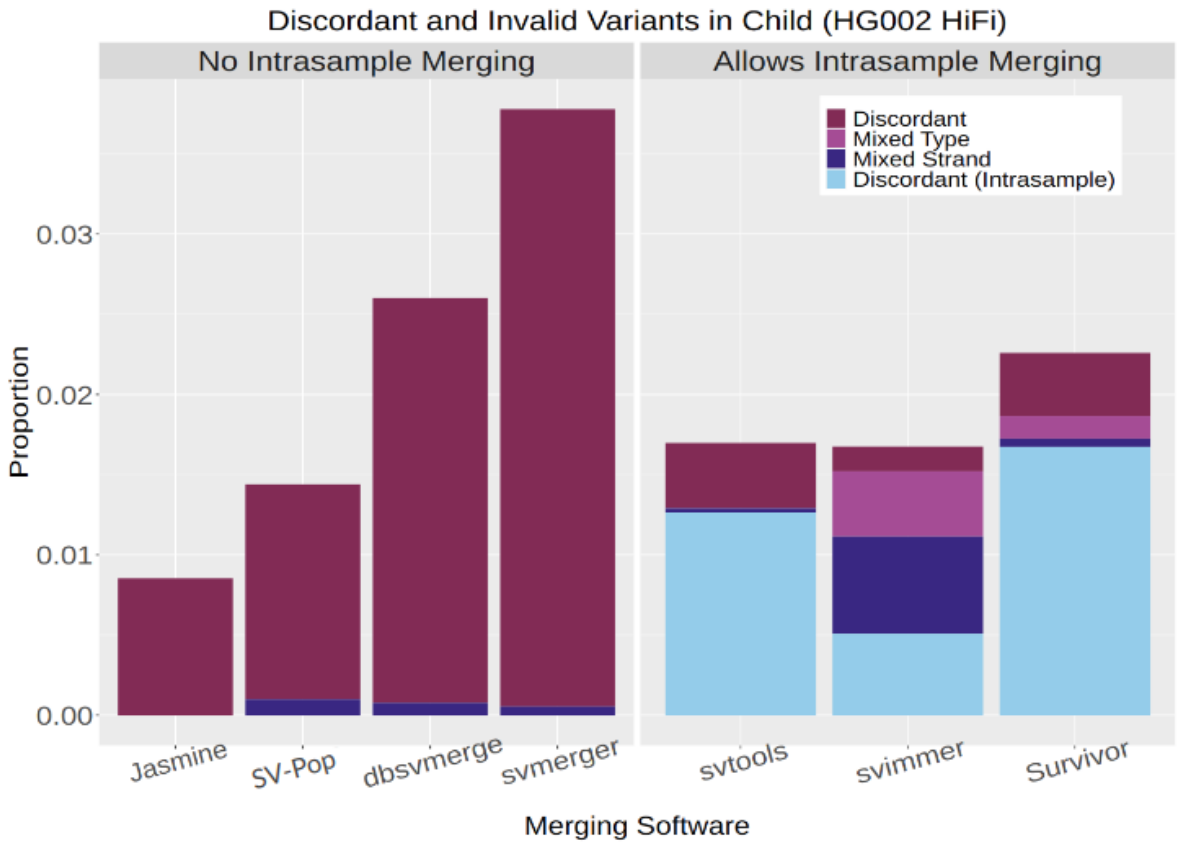

Supplementary Figure 4. Discordance in HG002 of All Merging Software for SVs and Indels
The rate of discordance when comparing SVs and indels between individuals with Jasmine as well as six existing methods for population inference.

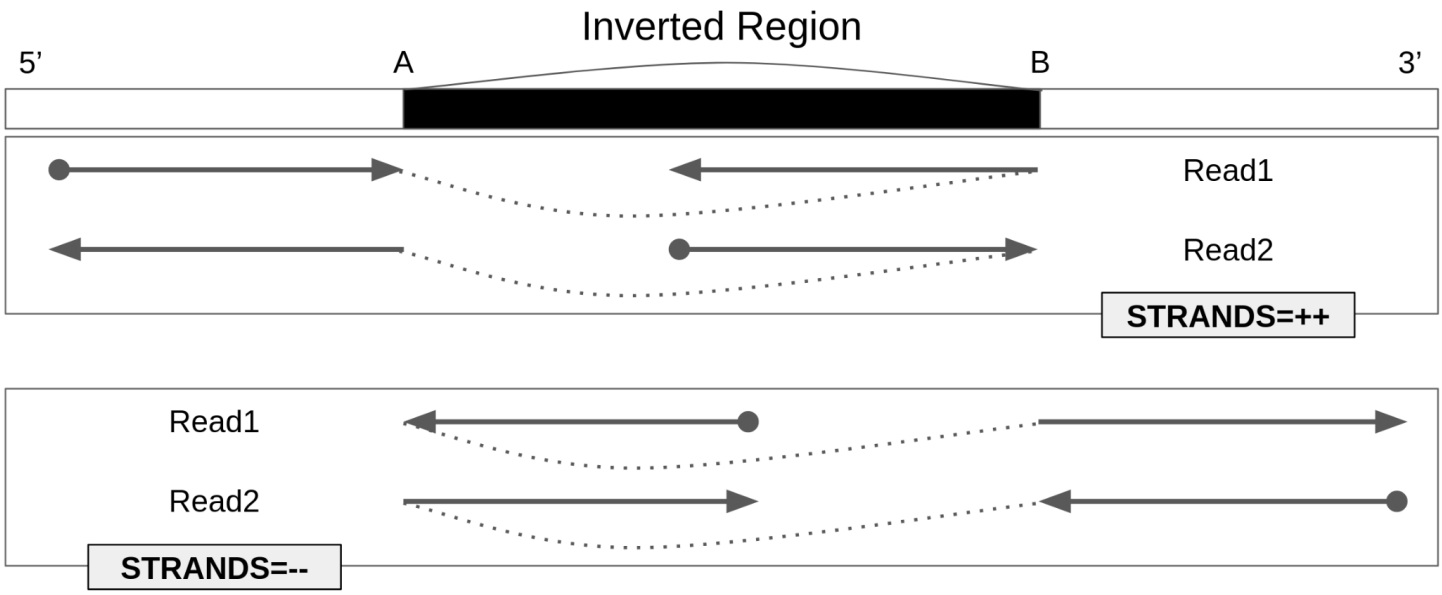

Supplementary Figure 5. Example of Breakpoint Directionality.
In complex regions with nested SVs, some variant types such as inversions and translocations, which typically correspond to two novel breakpoint adjacencies, may only be partially present due to other variants interacting with that one. In the case of inversions, one novel adjacency is that of the start of the inverted region to downstream sequence, and the other is that of the end of the inverted region to upstream sequence, This example shows an inversion where there are two novel breakpoint adjacencies; 1) the sequence near A going towards the 5’ end being newly adjacent to the sequence near B going towards the 5’ end (denoted by STRANDS=++), and 2) the sequence near A going towards the 3’ end being newly adjacent to the sequence near B going towards the 3’ end (denoted by STRANDS=--). While these novel adjacencies typically co-occur, it is necessary to distinguish which is present in the case where only one occurs. While some SV callers collapse these adjacencies into a single SV call, they are reported by sniffles as distinct SV calls with different values for the STRANDS INFO field, and downstream SV comparison/merging software must be aware of the difference between them when comparing across samples.

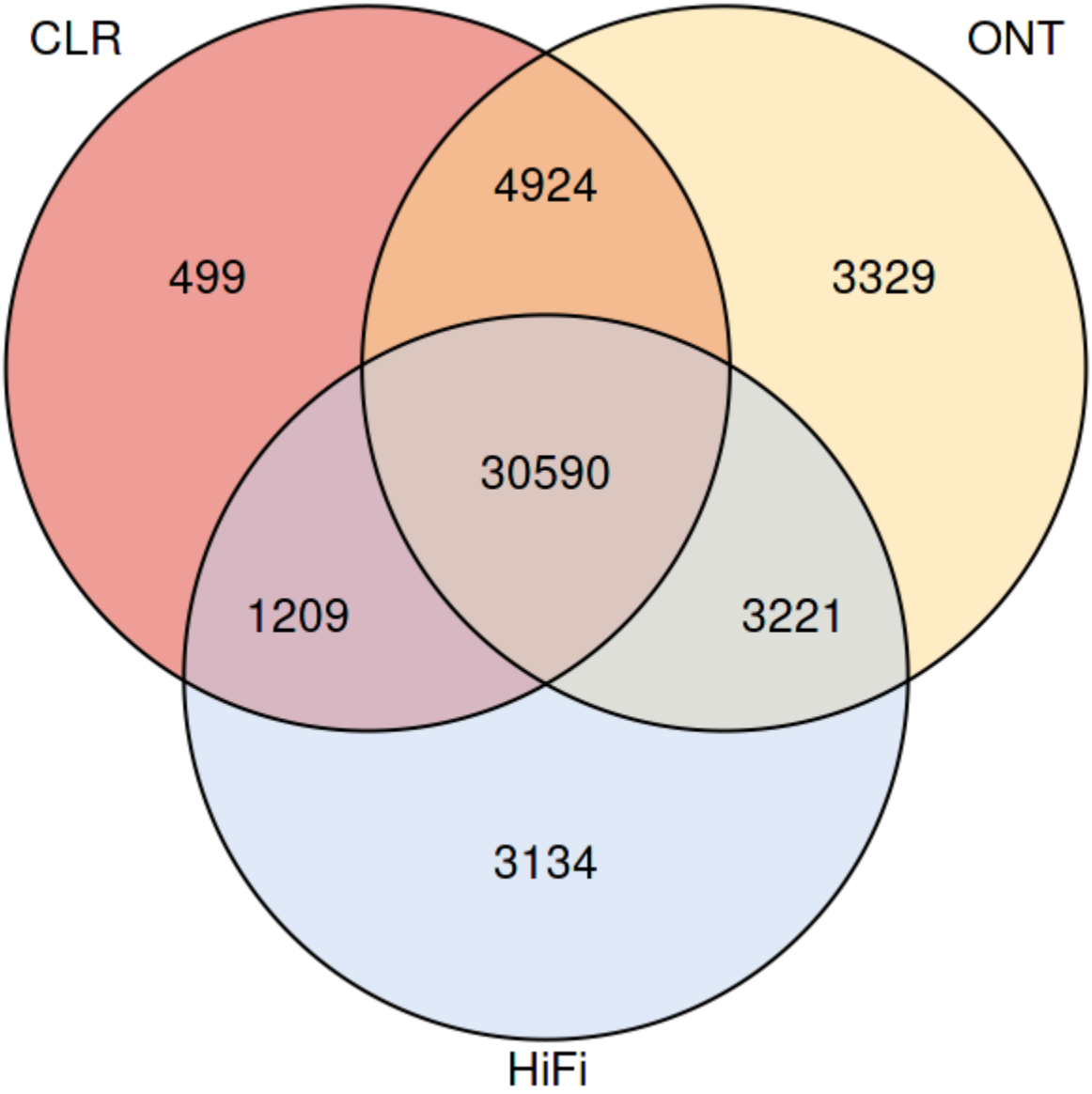

Supplementary Figure 6. HG002 Cross-Technology Agreement for SVs and Indels
This diagram shows the number of variants, including both SVs and indels, discovered by each subset of technologies when calling variants in HG002 from CLR, ONT. and HiFi reads.

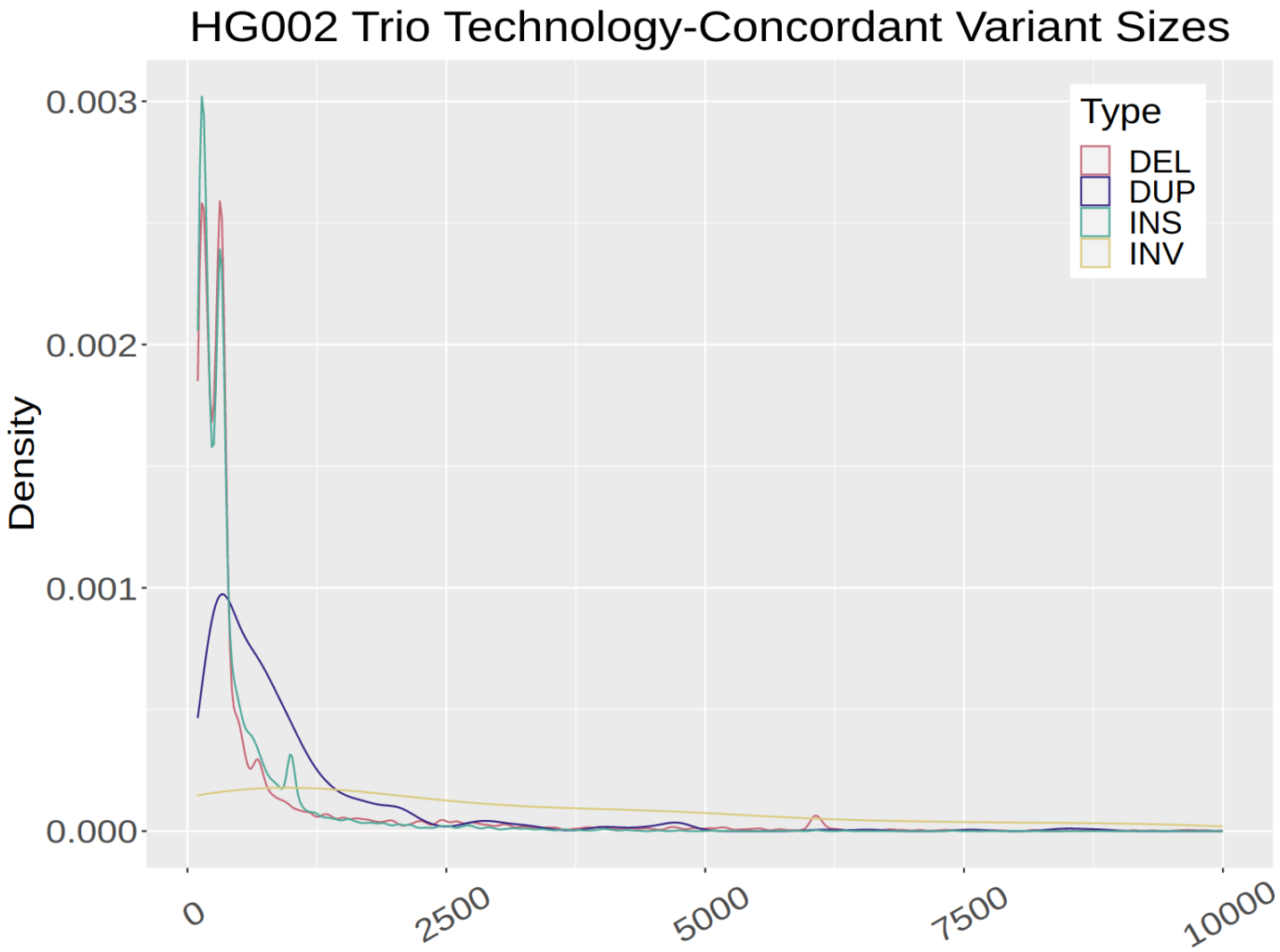

Supplementary Figure 7. HG002 Trio Technology-Concordant Variant Size Density
The density distribution of variant sizes called in the HG002 trio which are supported by HiFi, CLR, and ONT data. The spikes in the distribution around 300bp and 6-7kbp correspond to SINE and LINE elements, respectively.

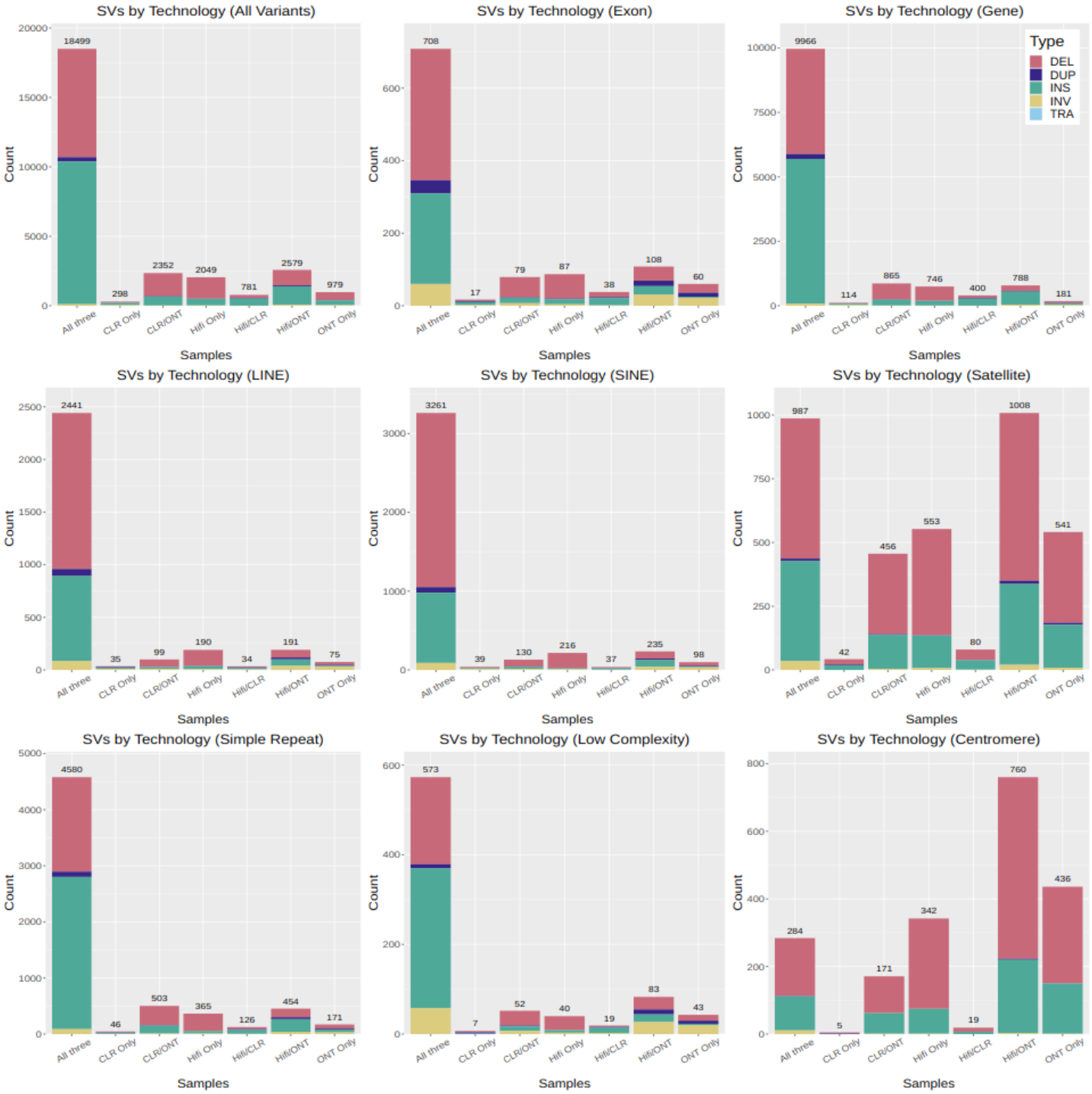

Supplementary Figure 8. HG002 Cross-Technology Agreement for SVs by Genomic Context.

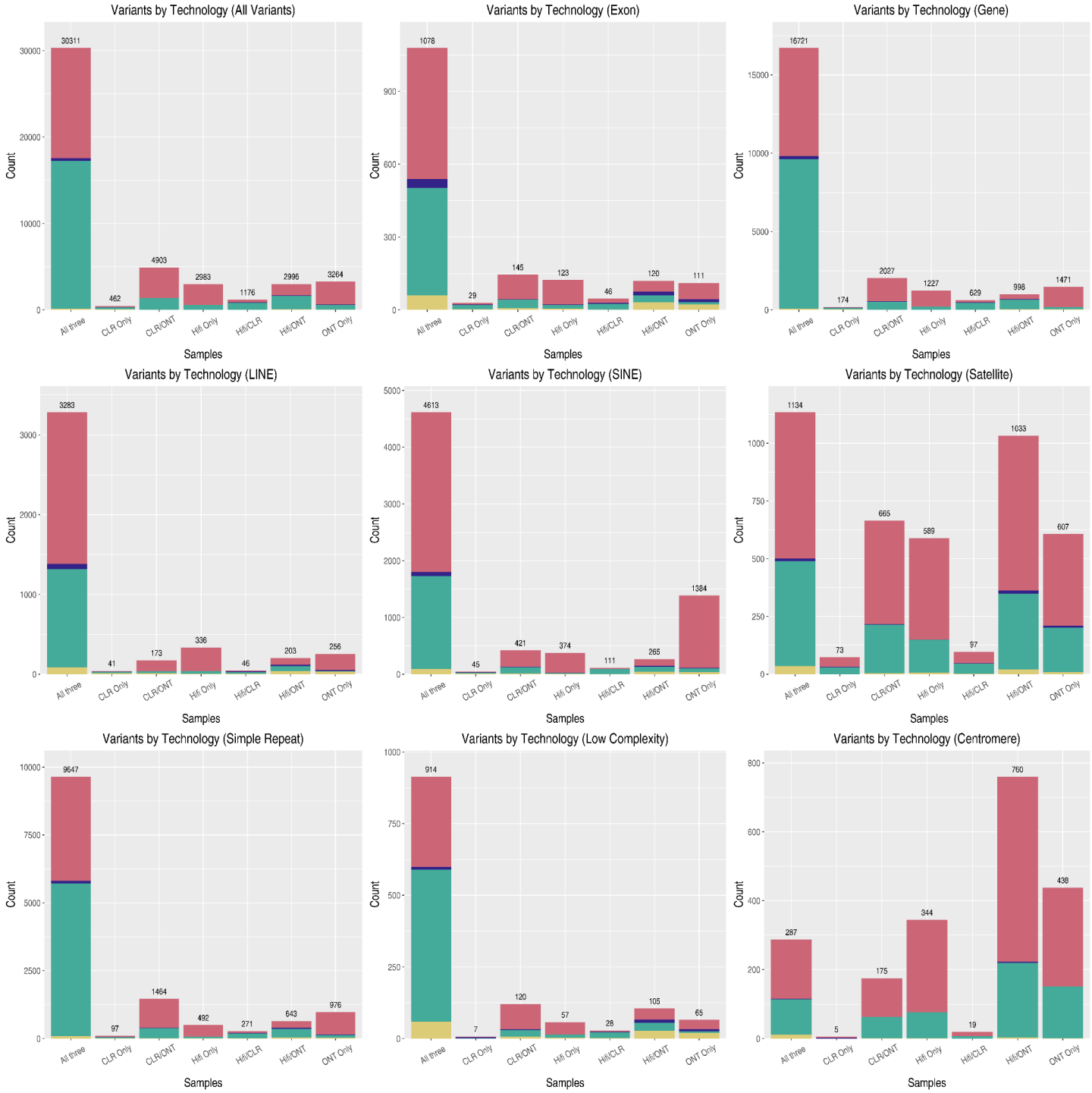

Supplementary Figure 9. HG002 Cross-Technology Agreement for SVs/Indels by Genomic Context.

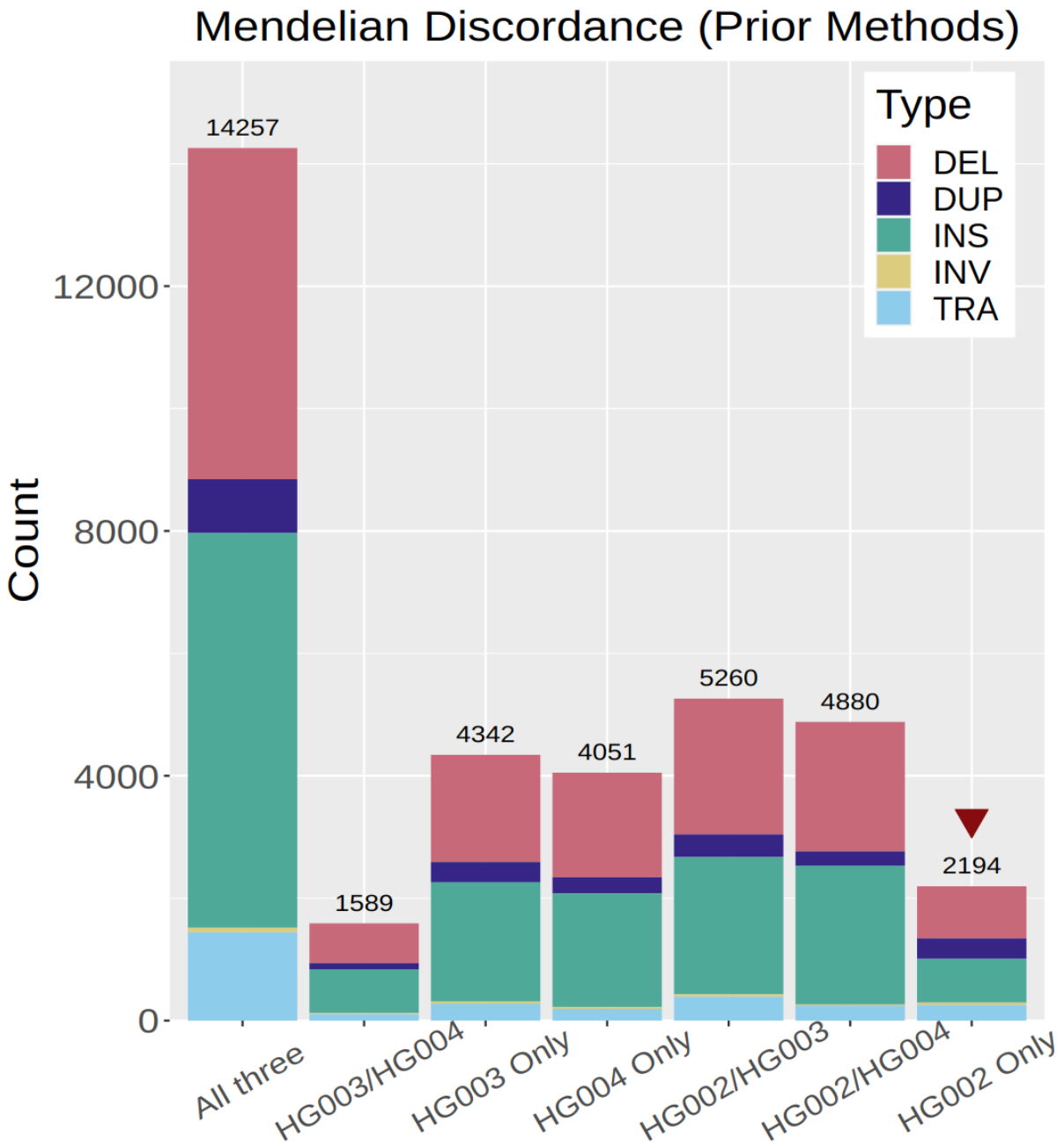

Supplementary Figure 10. Discordance in HG002 of Prior Methods for SVs and Indels
The number of SVs and indels called in each subset of individuals when using prior methods to call variants from HiFi data in the HG002 trio: ngmlr for alignment, Sniffles for SV calling, and SURVIVOR for consolidating SVs between samples.

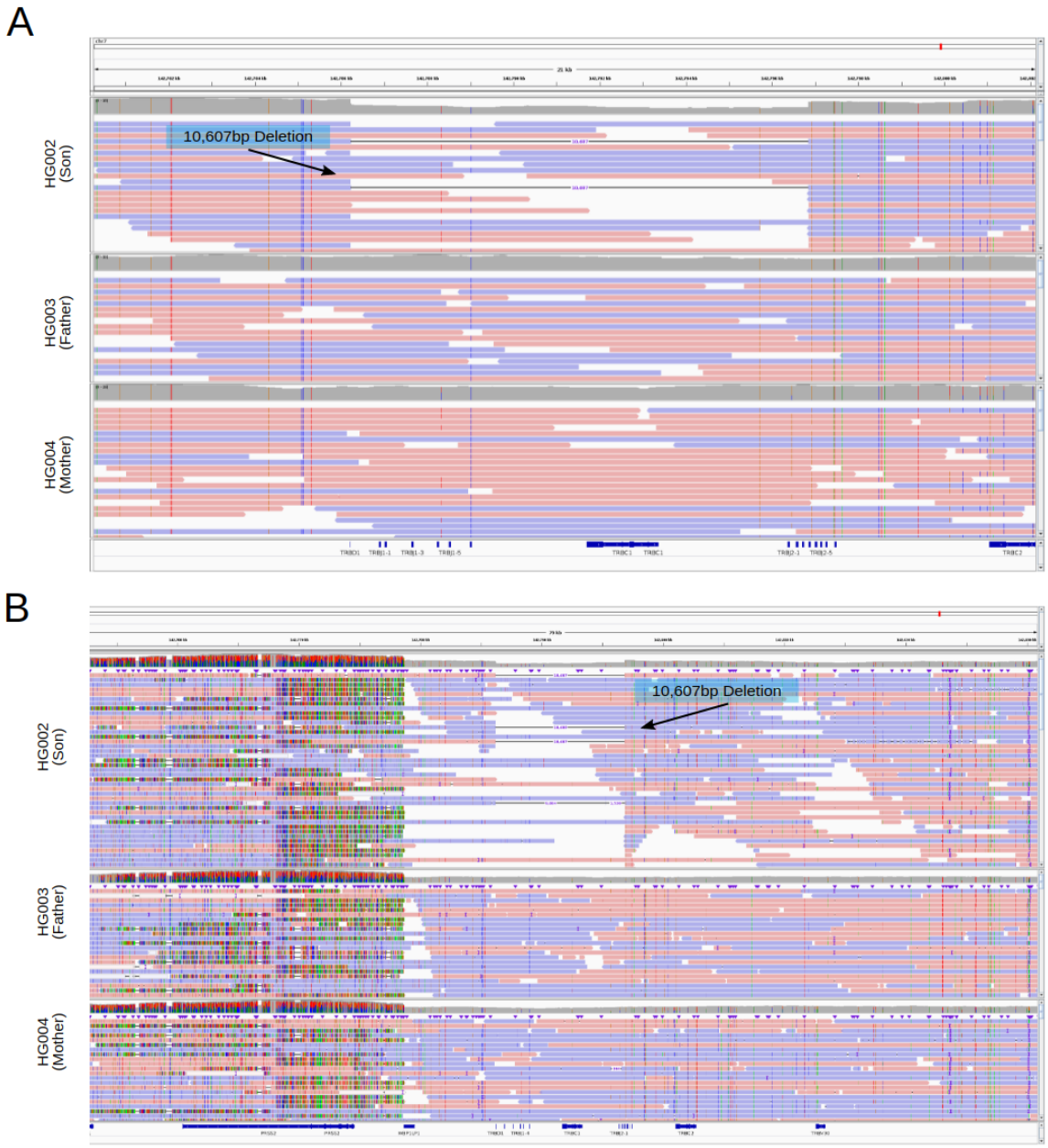

Supplementary Figure 11. Lower-Confidence Potential de novo SV in HG002.
This SV is supported by all three technologies as being present in HG002, and is a 10,607bp deletion at chr7:142786222, in the highly variable T cell Receptor Beta (TRB) region. **a.)** IGV screenshot showing the immediate context of the variant. **b.)** IGV screenshot which shows the highly variable region near the variant, leading us to be less confident of the variant being *de novo*.

A

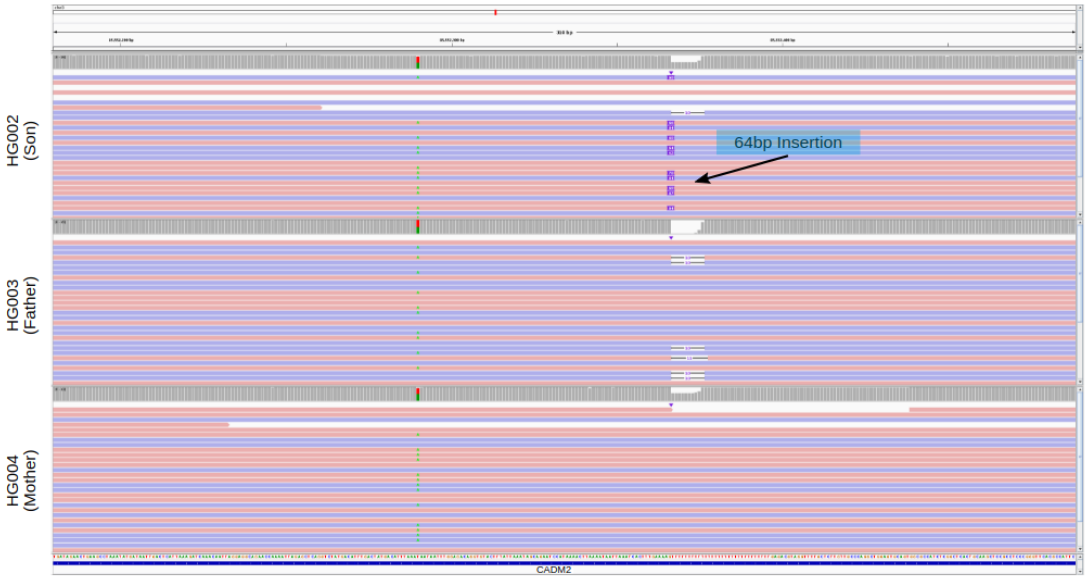

B

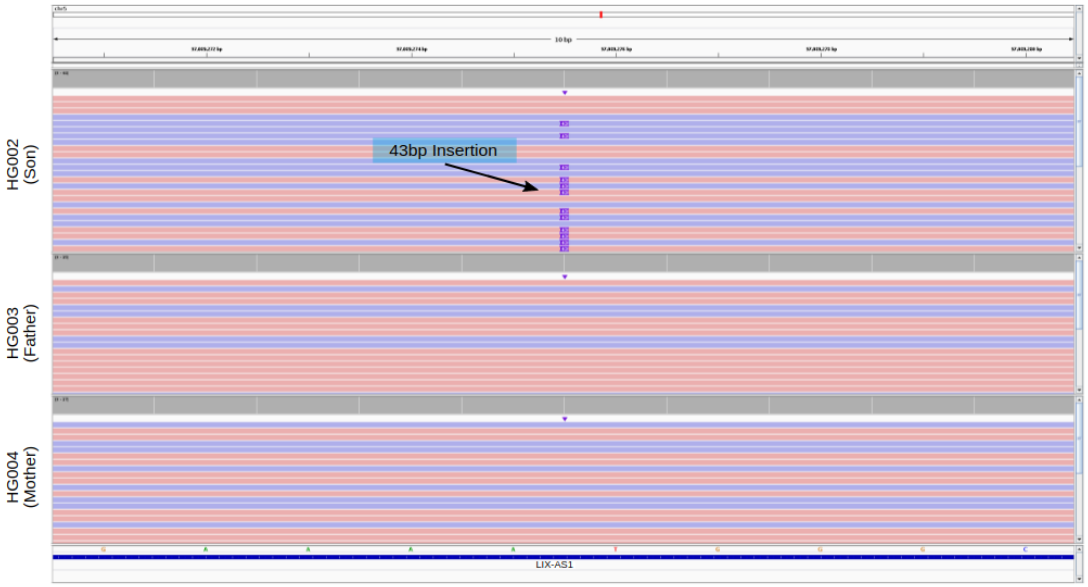

Supplementary Figure 12. Additional Potential de novo variants in HG002.
a.) A 64bp insertion at chr3:85552367. This variant was supported as being present in HG002 by HiFi and CLR reads, but missed by the ONT-based calls, likely due to the adjacent homopolymer.
b.) A 43bp insertion at chr5:97089276 supported by all three technologies.

A

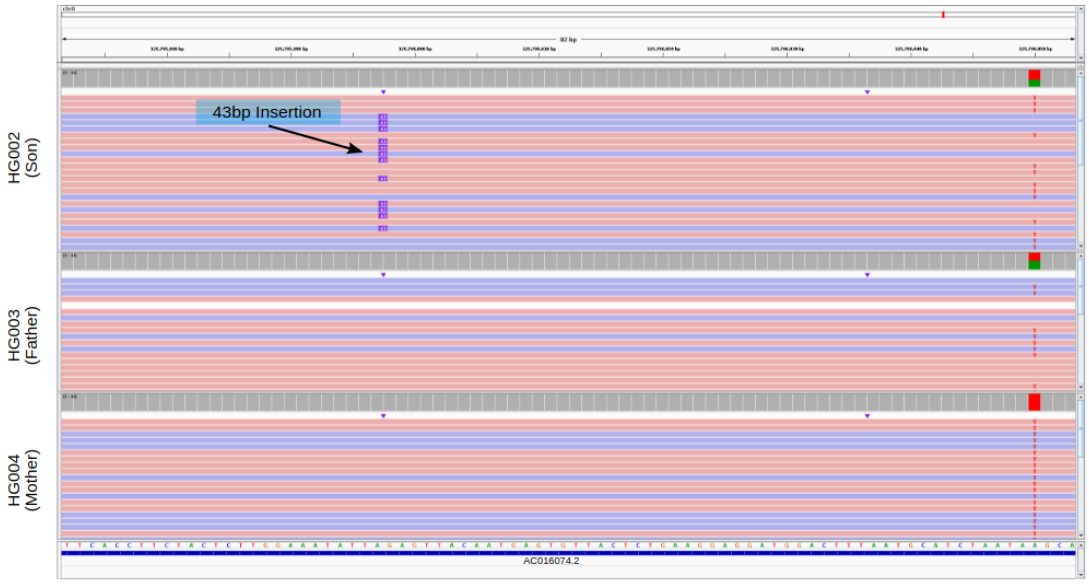

B

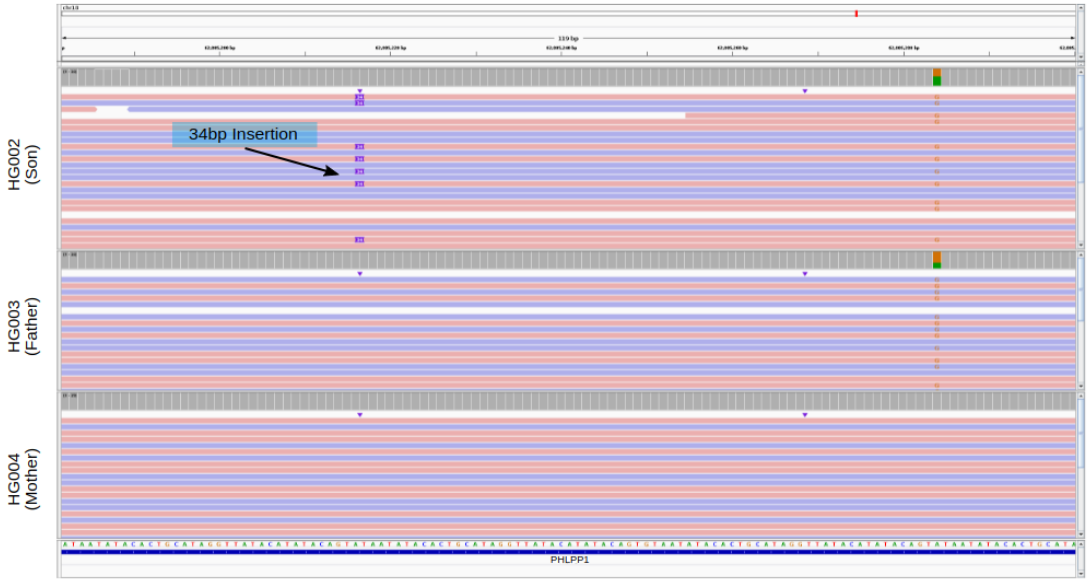

Supplementary Figure 13. Additional Potential de novo variants in HG002.
a.) A 43bp insertion at chr8:125785998 on the paternal haplotype supported by all three technologies.
b.) A 34bp insertion at chr18:62805217 on the paternal haplotype. This variant was supported as being present in HG002 by HiFi and ONT reads, but missed by the CLR-based calls.

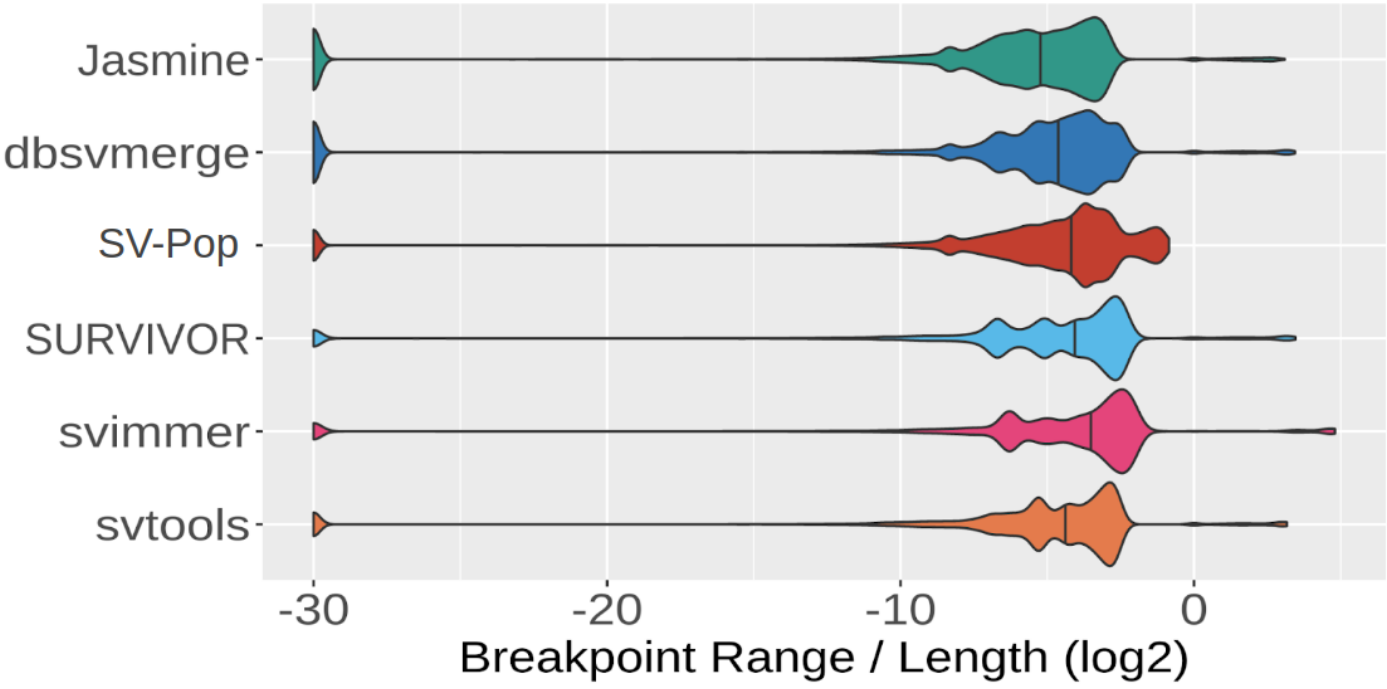

Supplementary Figure 14. Breakpoint Range in Cohort as Proportion of Length
The distribution of the range of breakpoints of variant calls merged into single variants by each software, excluding unmerged variants, when merging SVs and indels in our cohort of 31 samples of diverse ancestry.

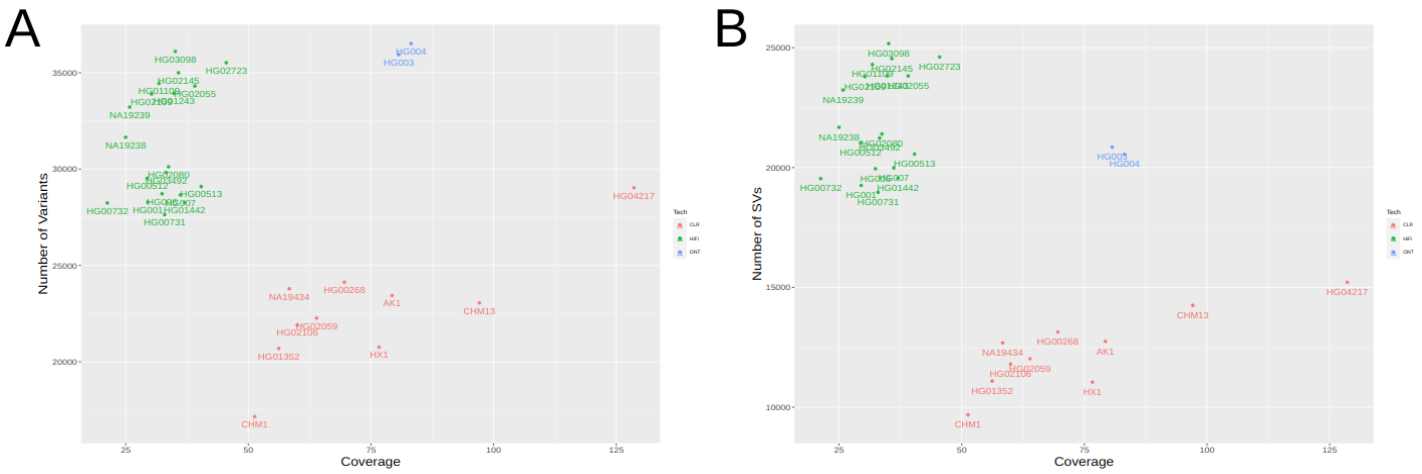

Supplementary Figure 15. Variant Counts per Sample.
This shows **a.)** the number of high-confidence variants called in each sample, including both SVs and indels, and **b.)** the number of SVs called in each sample. While most samples sequenced from the same technology have similar numbers of variants, the coverage of a sample, particularly in those sequenced with CLR, is positively associated with the number of variants detected.

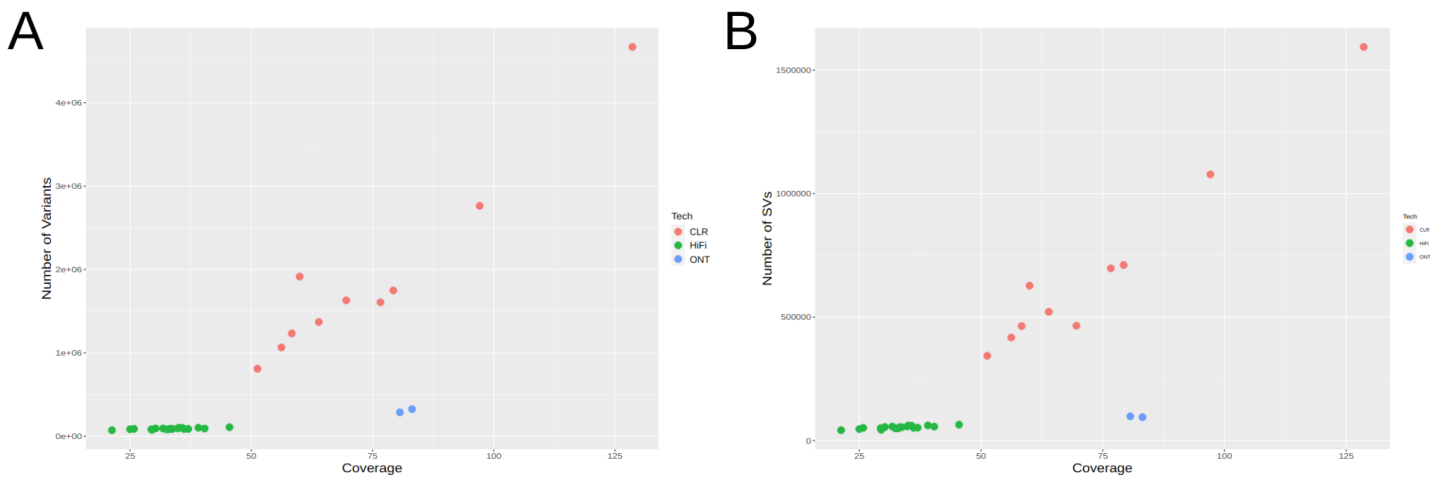

Supplementary Figure 16. Variant Counts per Sample including Low-Confidence Variants.
This shows **a.)** the number of variants called in each sample with a highly sensitive threshold, including both SVs and indels, and **b.)** the number of SVs called in each sample with a highly sensitive threshold. There is a high enrichment of low-confidence calls in samples sequenced with CLR, especially samples with high coverage, due to the technology's higher error rate.

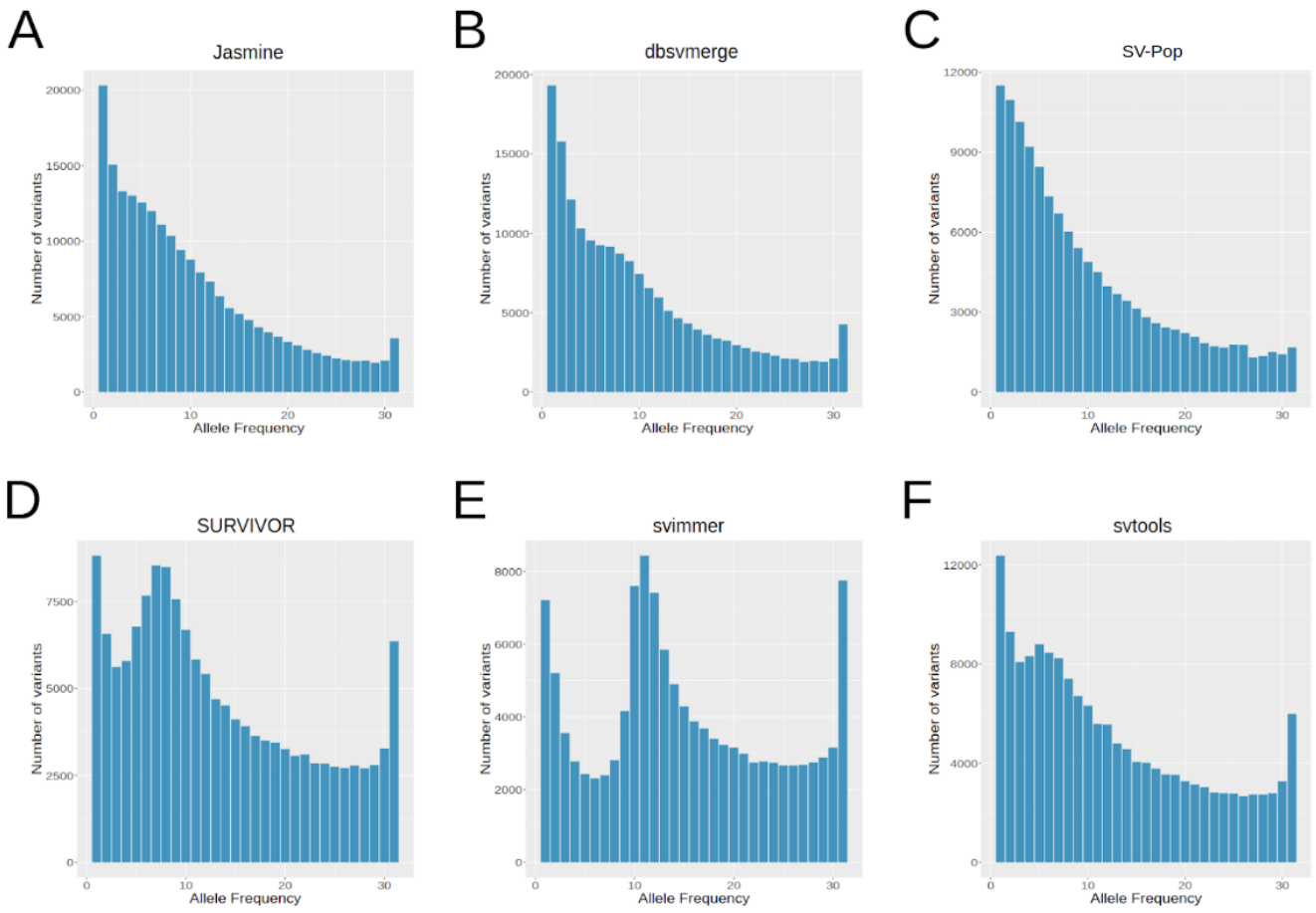

Supplementary Figure 17. Variant Allele Frequencies of all Merging Software.
The allele frequency distribution of SVs and indels in the 31-sample cohort when using different methods for merging calls across samples: **a.)** Jasmine **b.)** dbsvmerge **c.)** svpop **d.)** SURVIVOR **e.)** svimmer **f.)** svtools. When using methods which use a constant distance threshold for merging (SURVIVOR, svimmer, svtools), we observe a spike in the allele frequency distribution near 10 samples, where false positive calls from CLR-sequenced samples are merged with each other and with high-confidence variants in other samples.

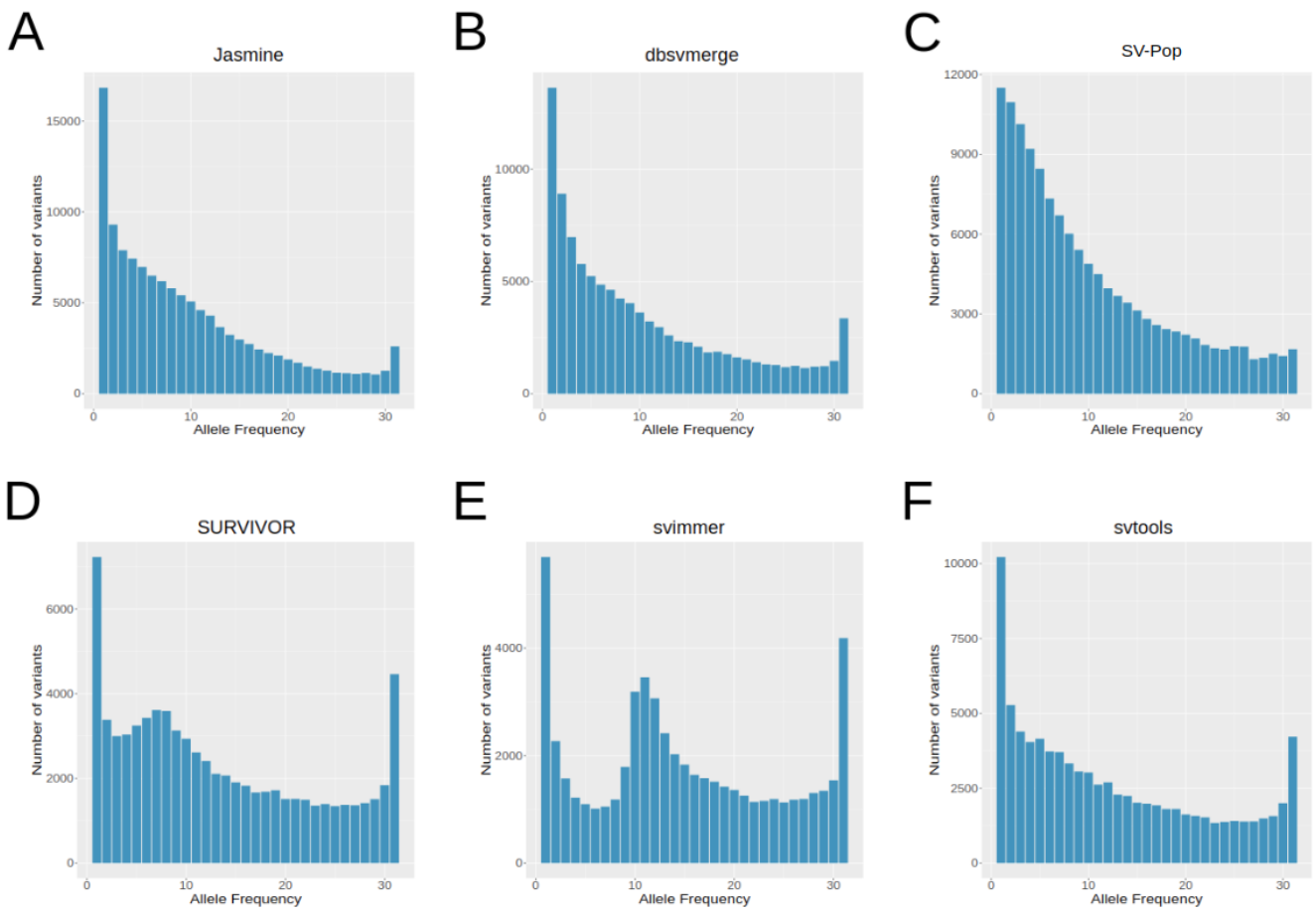

Supplementary Figure 18. SV Allele Frequencies of all Merging Software.

The allele frequency distribution of SVs of length at least 50bp in the 31-sample cohort when using different methods for merging calls across samples: a.) Jasmine b.) dbsvmerge c.) svpop d.) SURVIVOR e.) svimmer f.) svtools.

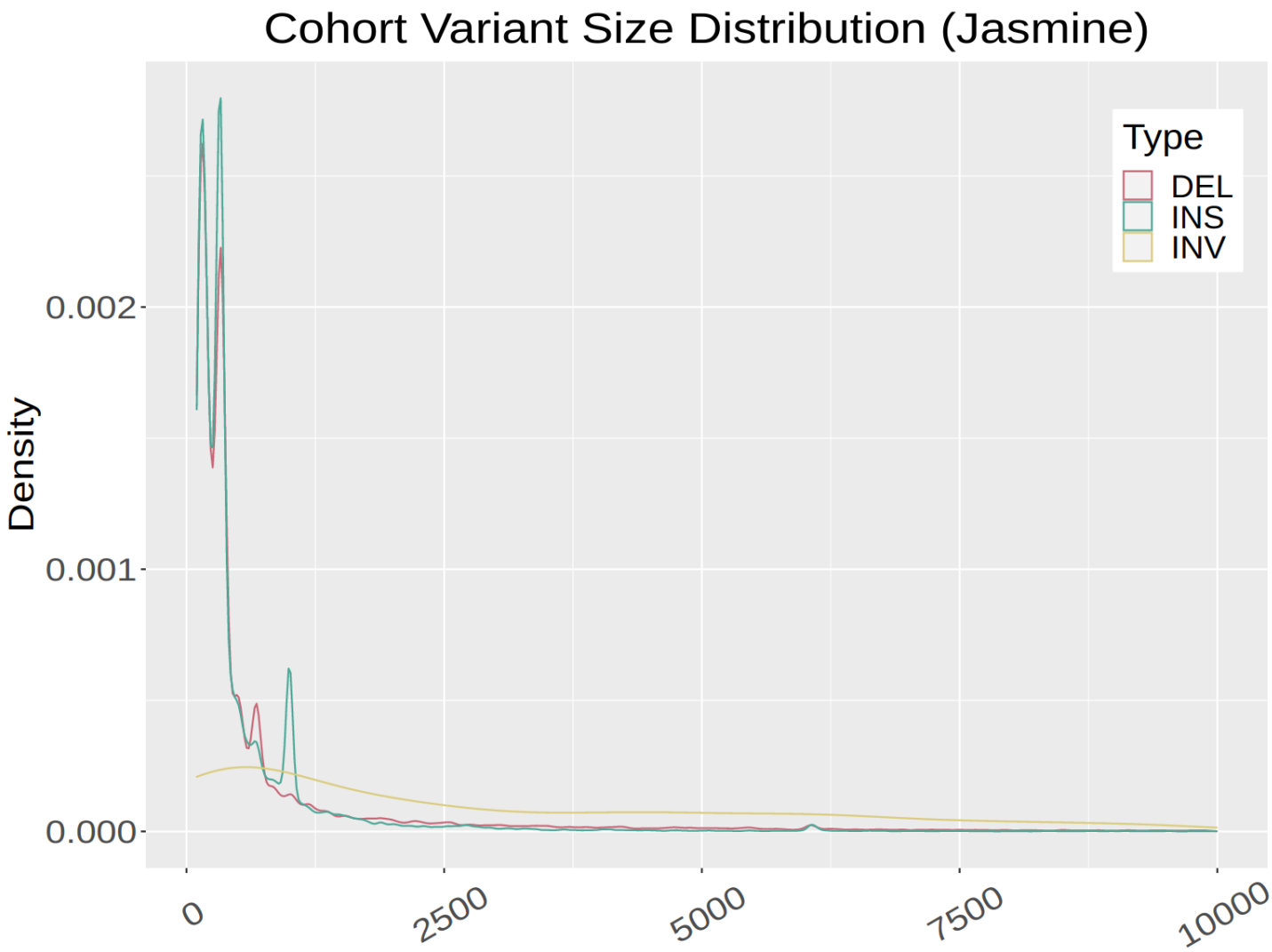

Supplementary Figure 19. Cohort Variant Size Density

The density distribution of variant sizes called in the 31-sample cohort. The spikes in the distribution around 300bp and 6-7kbp correspond to SINE and LINE elements, respectively.

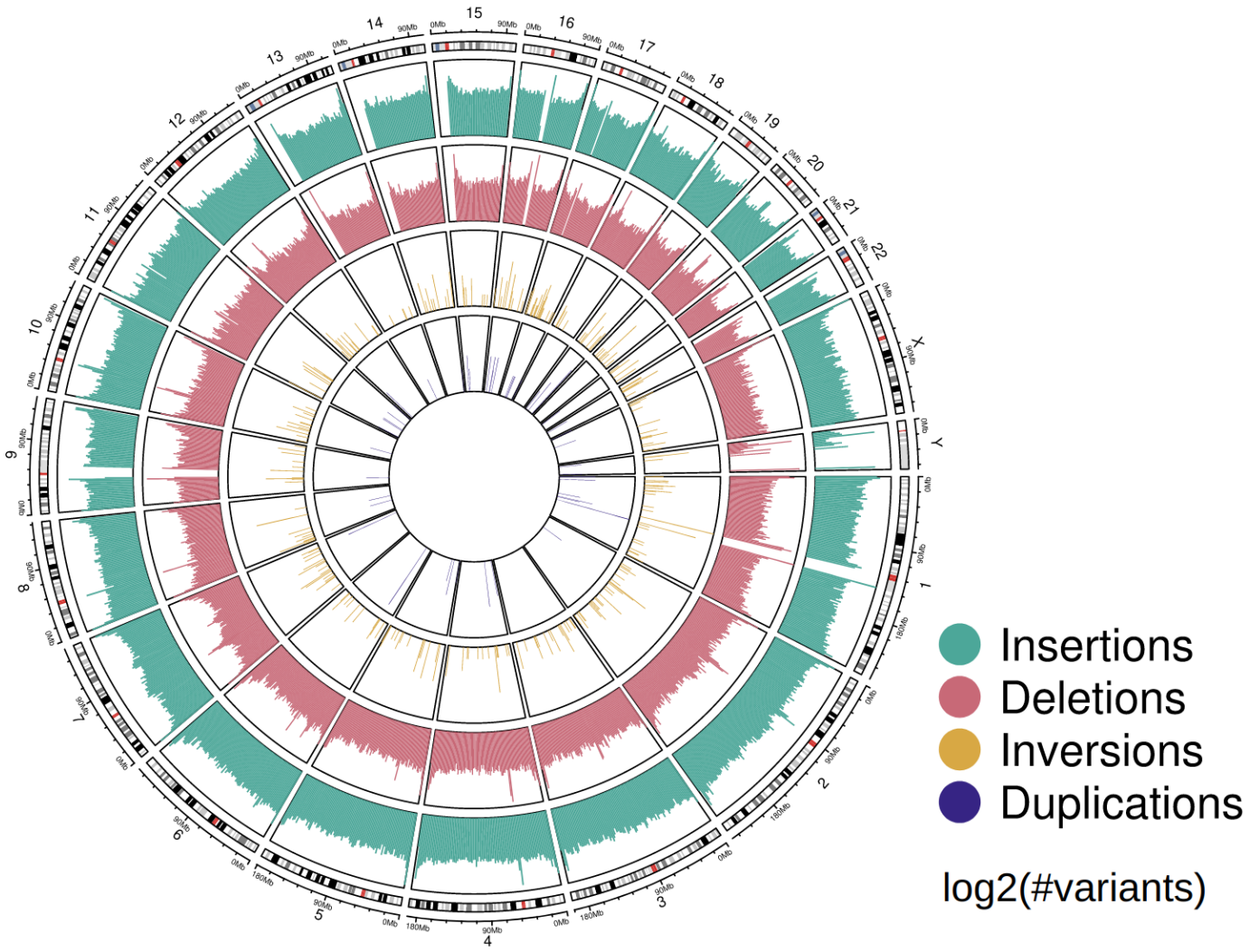

Supplementary Figure 20. Genomic Positions of SVs and Indels in Cohort

This shows the number of SVs and indels in the cohort in 1Mbp bins across the human genome in the cohort of 31 samples.

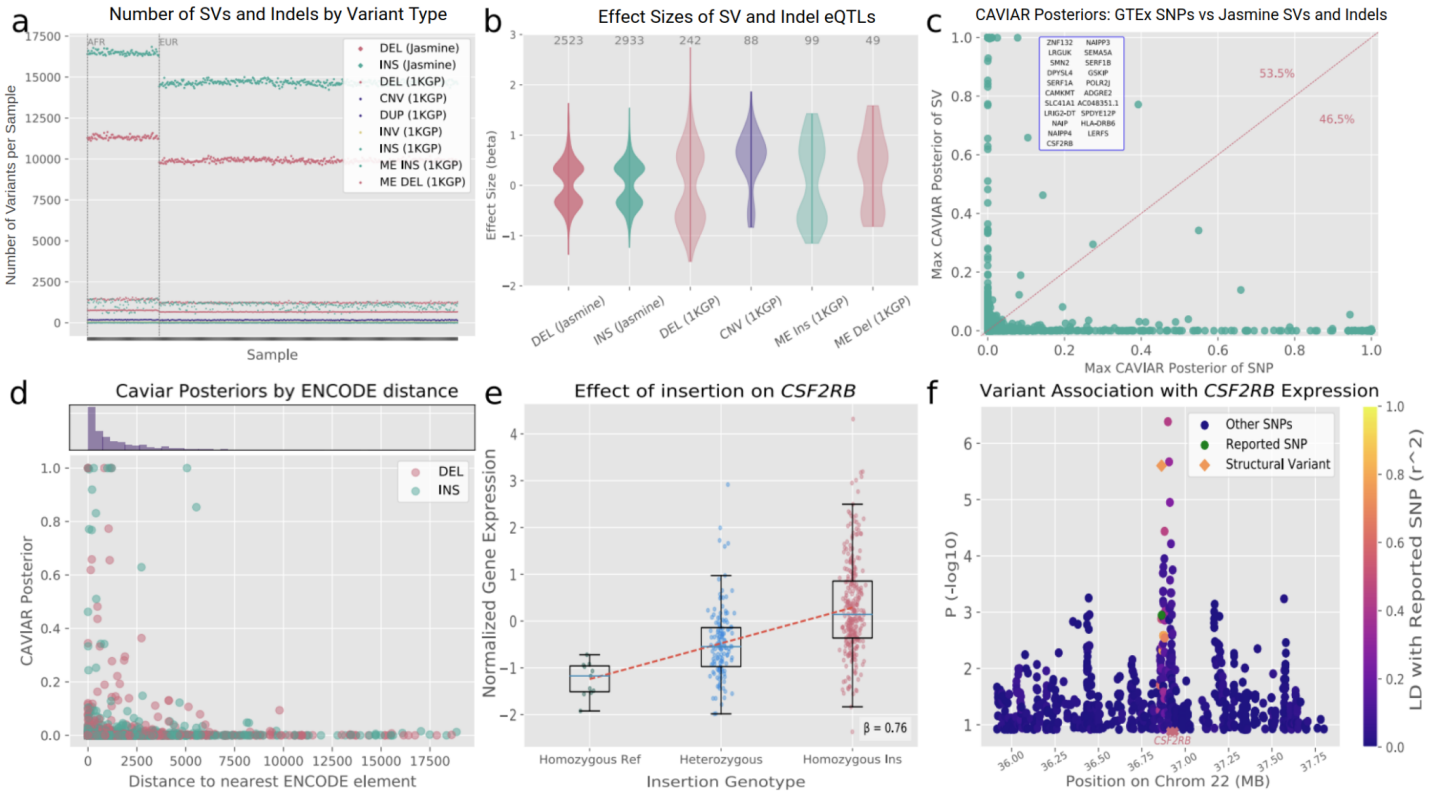

Supplementary Figure 21. Functional impact of SVs and indels from Jasmine in 1KGP samples

We used Paragraph to genotype SVs and indels from the cohort of 31 samples in 444 samples from the 1000 Genomes Project which have RNA-seq data. **a.)** Number of variants detected per sample for genotyped SVs and indels (Jasmine) versus SVs reported in the 1000 Genomes Project (1KGP) after HWE filtering. **b.)** Effect sizes of significant SV and indel eQTLs mapped from Jasmine variants or 1KGP SVs. **c.)** CAVIAR posterior probabilities for each gene with significant SV/indel and SNP data. The x-axis is the maximum CAVIAR posterior of a SNP reported as a SNP-eQTL by the GTEx consortium, and the y-axis is the maximum CAVIAR posterior of a Jasmine variant from our mapped SV and indel eQTLs. Variants above the diagonal line have a higher Jasmine variant posterior than GTEx SNP posterior. The inset box contains genes with highly causal (posterior >0.8) SVs. **d.)** Jasmine variant distance to the nearest ENCODE cCRE versus CAVIAR posterior. The histogram shows the distribution of distances to ENCODE cCREs. **e.)** Genotype and gene expression distribution in 1KGP samples for novel *CSF2RB*-associated insertion (n=444). **f.)** Manhattan plot for SNPs and the novel SV near *CSF2RB*, with p-value measured by one-sided Wilcoxon rank-sum test. The green point is the SNP reported in GTEx eQTLs (chr22_36864559_A_G); other points are colored by LD to that SNP. For e and f, one-sided Wilcoxon Rank Sum test was performed to assess the p-values of variant-gene association. We corrected for multiple hypothesis using gene level Bonferroni test at FDR 10%. The boxplot's lower bound is 1st quartile and the upper bound is 3rd quartile. And the whiskers are at +/- 1.5 interquartile range from the 1st or 3rd quartile. and the center is the mean expression level of a genotype group.

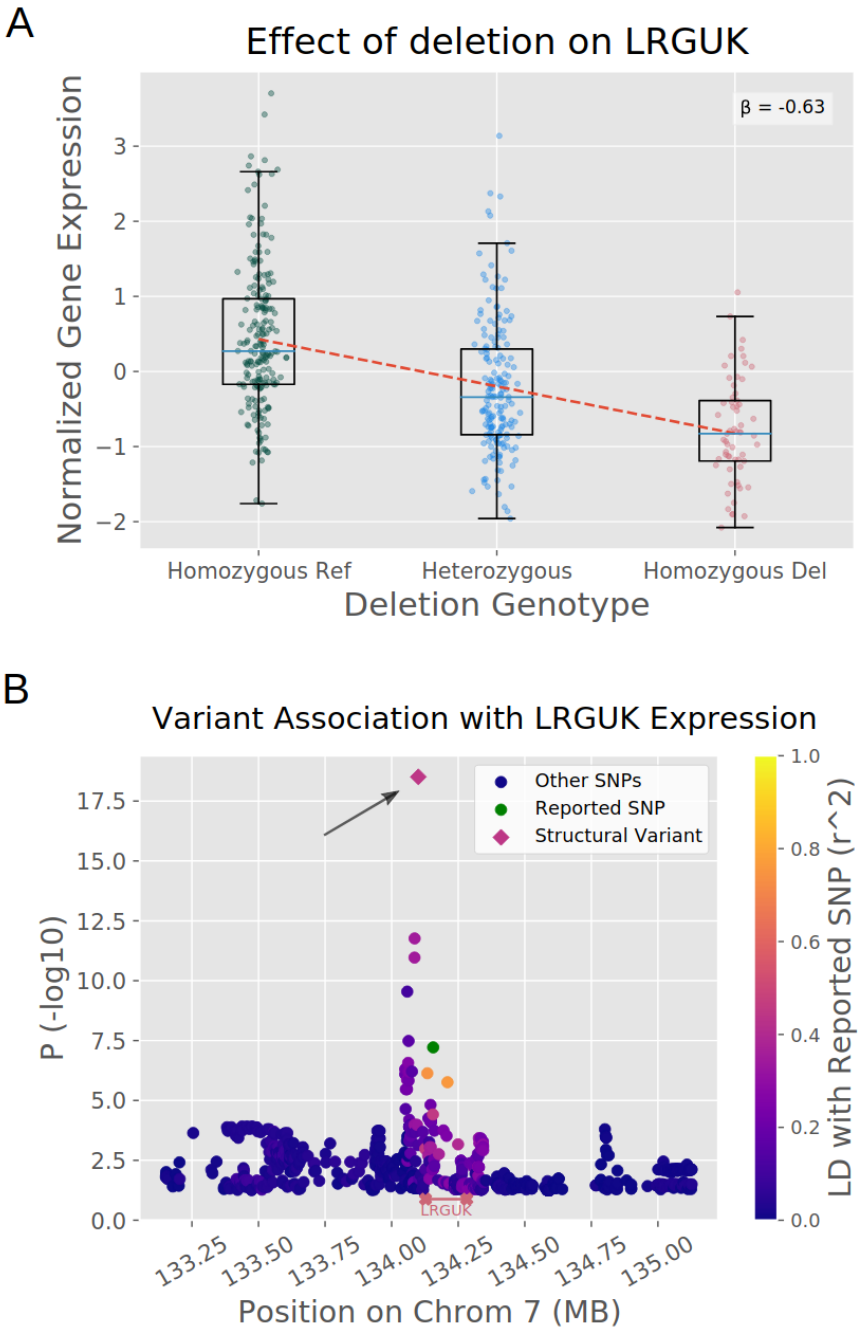

Supplementary Figure 22. Potential Functionally Relevant Deletion in LRGUK in 1KGP.
Deletion in *LRGUK* genotyped with Jasmine in 1KGP samples in LD with reported GWAS SNP. **a.)** Genotype versus gene expression among the 1000 Genomes Project samples for the deletion in *LRGUK* (n=444). **b.)** Manhattan plot for SNPs and SV near *LRGUK*, with p-value measured by one-sided Wilcoxon rank-sum test. The green point is the SNP reported in GWAS to be associated with smoking initiation (rs1561112), and other points are colored by LD to that SNP. For A and B, one-sided Wilcoxon Rank Sum test was performed to assess the p-values of variant-gene association. We corrected for multiple hypothesis using gene level Bonferroni test at FDR 10%. The boxplot's lower bound is 1st quartile and the upper bound is 3rd quartile. And the whiskers are at +/- 1.5 interquartile range from the 1st or 3rd quartile. and the center is the mean expression level of a genotype group.

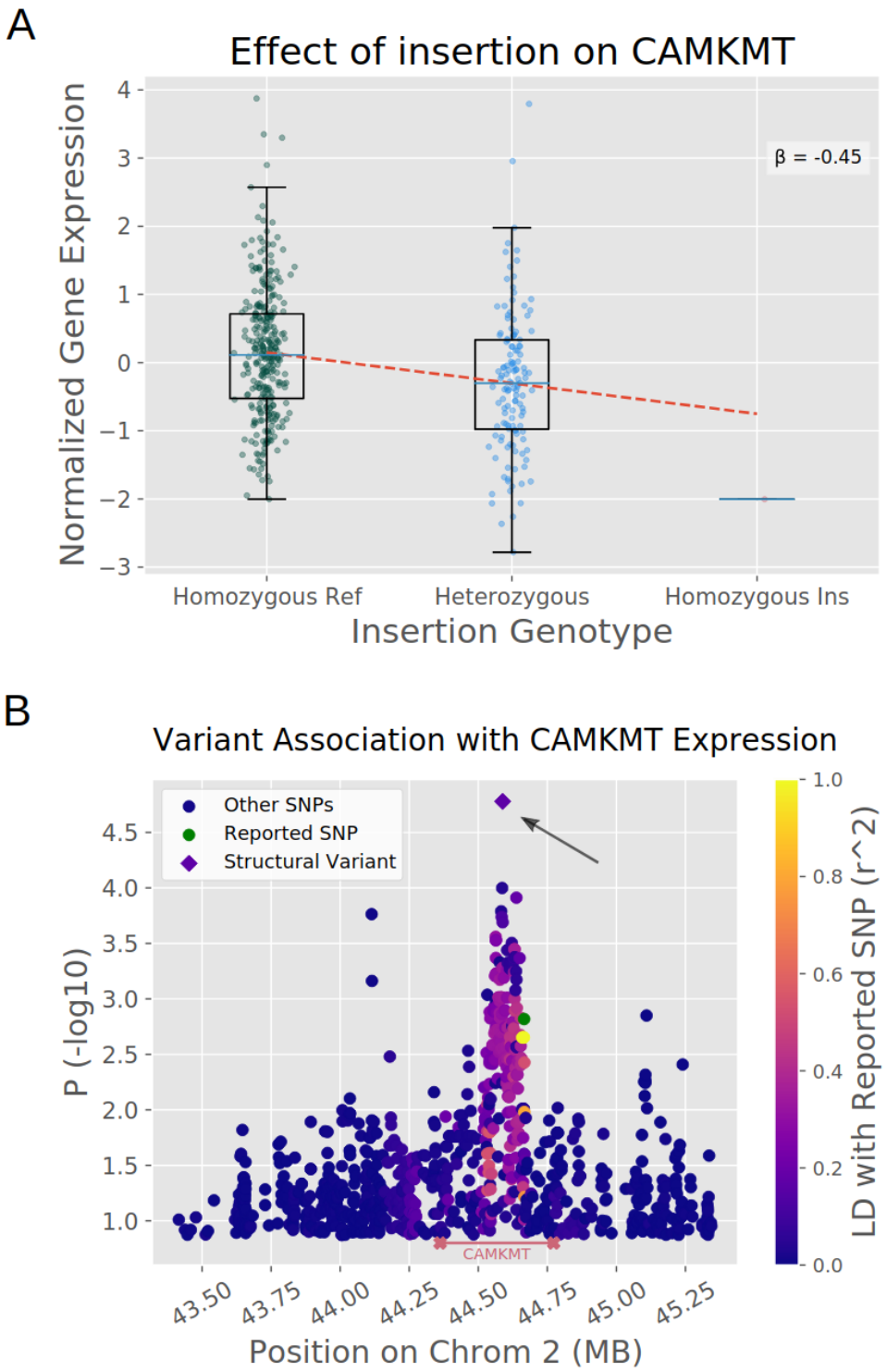

Supplementary Figure 23. Potential Functionally Relevant Insertion in CAMKMT in 1KGP. Insertion in *CAMKMT* genotyped with Jasmine in 1KGP samples in LD with reported SNP-eQTLs. **a.)** Genotype versus gene expression among the 1000 Genomes Project samples for the insertion in *CAMKMT* (n=444). **b.)** Manhattan plot for SNPs and SV near *CAMKMT*, with p-value measured by one-sided Wilcoxon rank-sum test. The green point is the SNP-eQTL from GTEx (chr2_44665995_C_T), and other points are colored by LD to that SNP. For A and B, one-sided Wilcoxon Rank Sum test was performed to assess the p-values of variant-gene association. We corrected for multiple hypothesis using gene level Bonferroni test at FDR 10%. The boxplot's lower bound is 1st quartile and the upper bound is 3rd quartile. And the whiskers are at +/- 1.5 interquartile range from the 1st or 3rd quartile. and the center is the mean expression level of a genotype group.

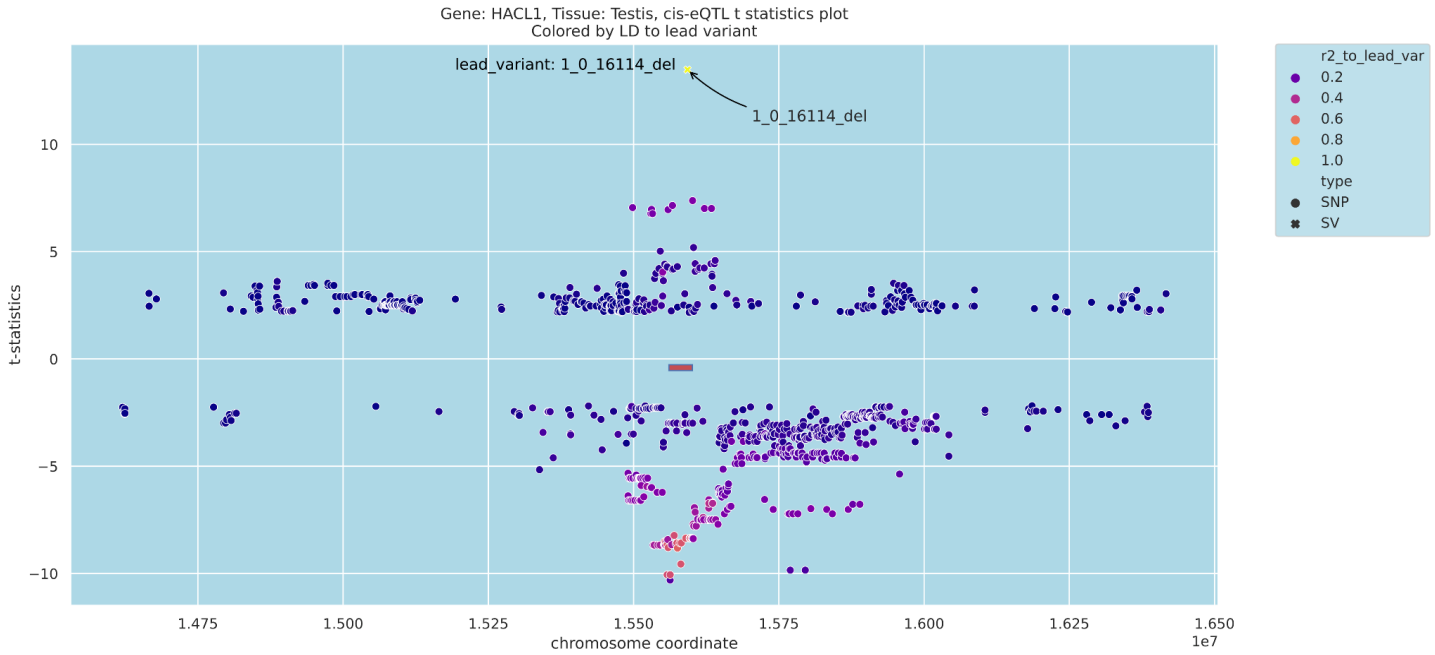

Supplementary Figure 24. Manhattan Plot of cis-eQTL association t-statistics for HACL1 in Testis

Manhattan plot for the t-statistic of SNPs and the SV near HACL1, with the t-statistic measured as the beta effect size divided by the variance of beta. The x-axis shows the position along chr3.

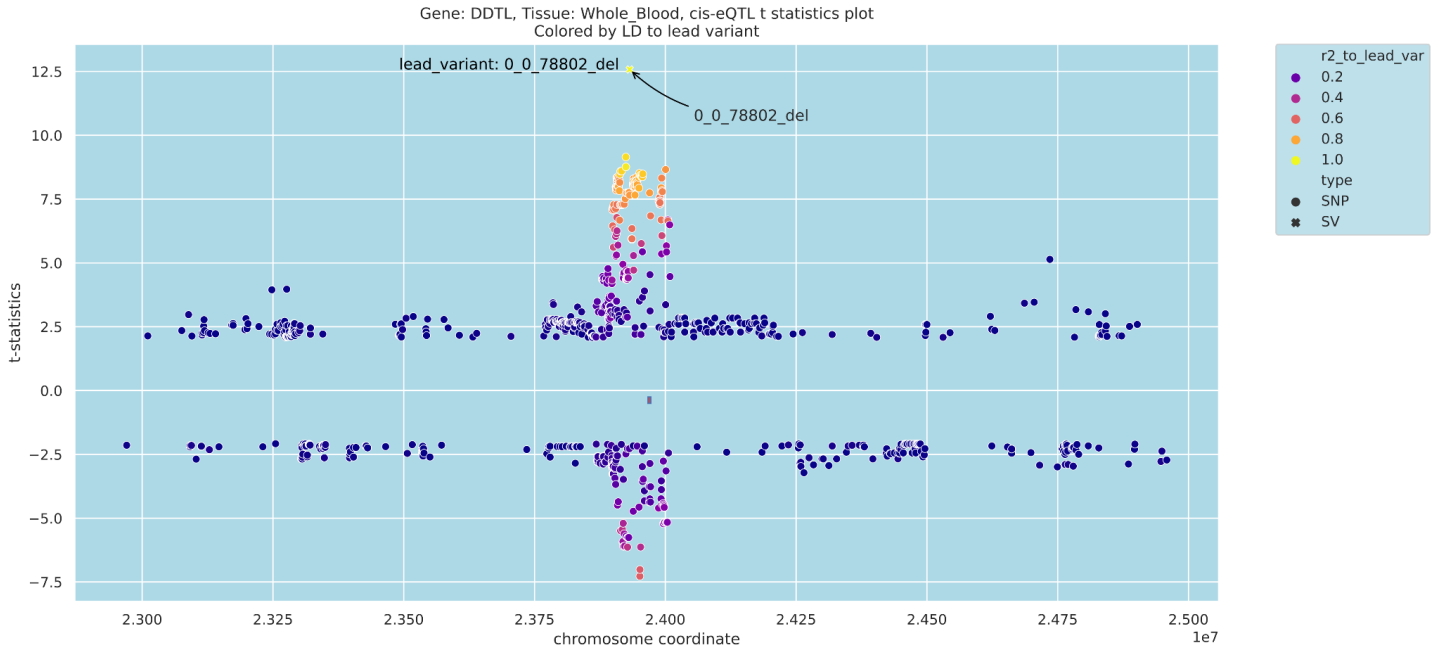

Supplementary Figure 25. Manhattan Plot of cis-eQTL association t-statistics for DDTL in Whole Blood

Manhattan plot for the t-statistic of SNPs and the SV near DDTL1, with the t-statistic measured as the beta effect size divided by the variance of beta. The x-axis shows the position along chr22.

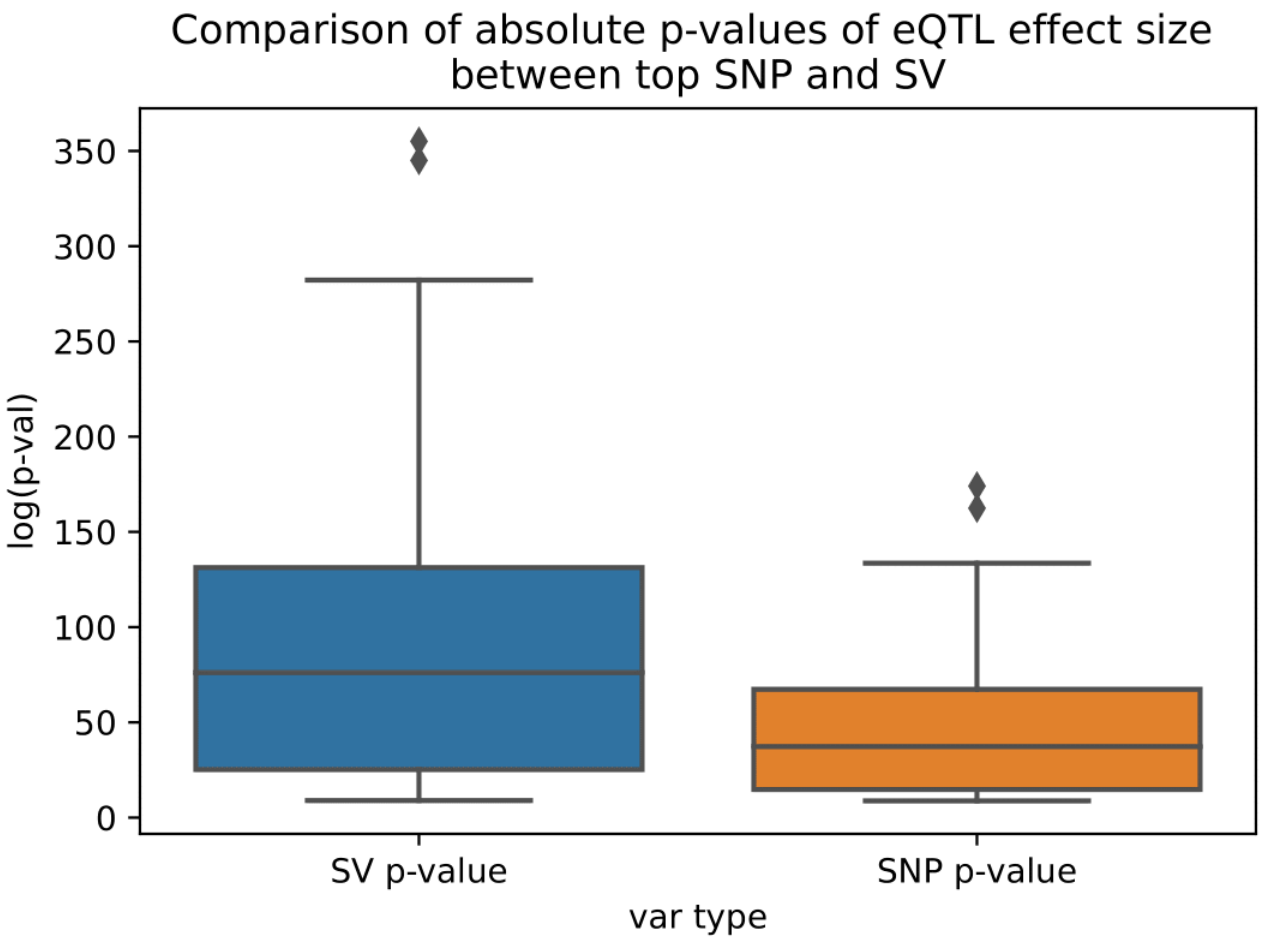

Supplementary Figure 26. Boxplot of the distributions of p-values for cis-eQTL associations across multiple tissues

For the DDTL SV-eQTL, we found the SV has the strongest CAVIAR posterior in 36 tissues. The left boxplot displays the distribution of the SV association p-values in these tissues, and the right boxplot displays GTEx v8 top SNP p-values. Comparing the SV p-value to corresponding top reported SNP p-value in matched tissue using one-sided Wilcoxon Rank Sum test, we found the SV p-values to be significantly higher than that of the SNPs with a p-value of 1.1e-8. This demonstrates that this SV is more likely to be the causal eQTL across tissues. The boxplot's lower bound is 1st quartile and the upper bound is 3rd quartile. And the whiskers are at +/- 1.5 interquartile range from the 1st or 3rd quartile. and the center is the mean -log10 p-values of each group. Points in diamiond shape are the outliers according to being greater than the 3rd Quartile + 1.5IQR rule.

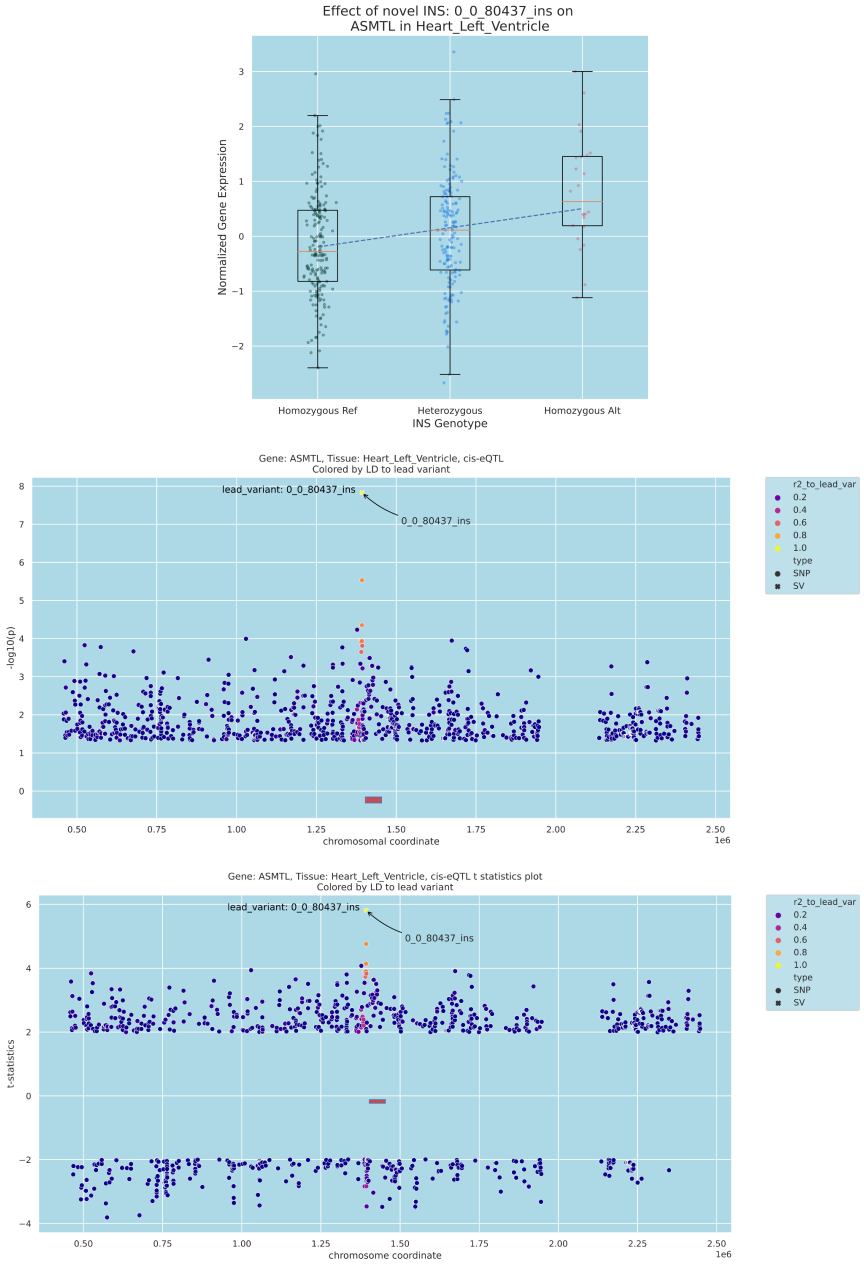

Supplementary Figure 27. SV-eQTL of ASMTL.

(top) Using our Jasmine-Paragraph pipeline in GTEx, we also identified a 60bp insertion on chromosome X that is an eQTL of ASMTL in GTEx heart left ventricle tissue (n=384). **(middle)** The insertion is in moderate LD (0.7 r^2) with the lead SNP-eQTLs but has a substantially stronger p-value of 1.5e-08 than the lead SNPs. The x-axis shows the position along chrX. **(bottom)** The insertion also has substantially stronger t-statistics of 5.81 in comparison to 4.14 of the lead SNP. The x-axis shows the position along chrX. For top, middle and bottom figures, two-sided t-test was performed to assess the p-values of variant-gene association. We corrected for multiple hypothesis using gene level Bonferroni test at FDR 5%. The middle plot is the negative log 10 p-values which are unsigned. And the bottom plots meant to show the direction of effect so t-statistics was used. The boxplot's lower bound is 1st quartile and the upper bound is 3rd quartile. And the whiskers are at +/- 1.5 interquartile range from the 1st or 3rd quartile. and the center is the mean expression level of a genotype group.

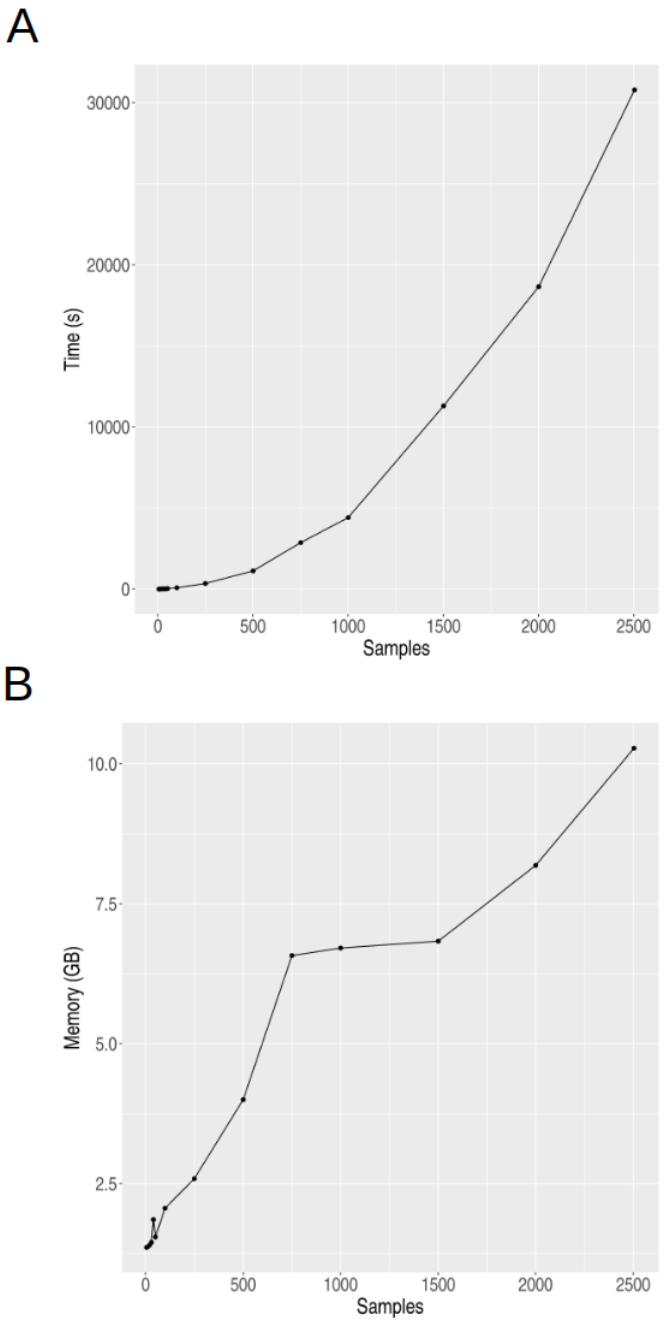

Supplementary Figure 28. Runtime and Memory on Large Simulated Datasets
a.) Runtime in seconds, and **b.)** Memory in GB required to merge simulated SV calls in different numbers of samples from the 1000 Genomes Project. Per-sample SVs were simulated based on the population-level Phase 3 structural variant dataset (https://www.internationalgenome.org/phase-3-structural-variant-dataset/) by consolidating all calls marked as present in that sample and shifting each of their start positions by a uniform random integer in [-50, 50].

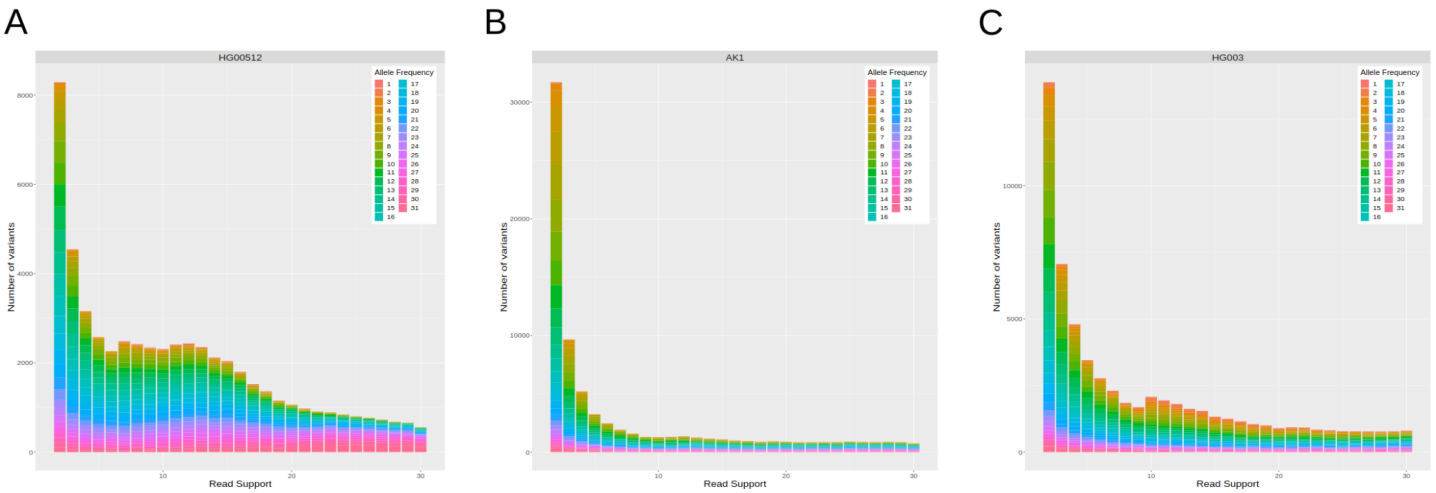

Supplementary Figure 29. Read Support across Sequencing Technologies.
In our population analysis, to examine the SV caller's ability to detect reads supporting variants across technologies, we measured the read support of each SV and indel for a representative sample sequenced with each technology. **a.)** HG00512, a HiFi sample with 29x average coverage. As expected, we see a sharp decrease at about 50% read support, corresponding to the transition from heterozygous to homozygous variants. **b.)** AK1, a CLR sample with 79x average coverage. In this sample, there are many variants supported by only a couple of reads, which is an artifact of reads having high sequencing error and moderate length. **c.)** HG003, an ONT sample with 81x average coverage.

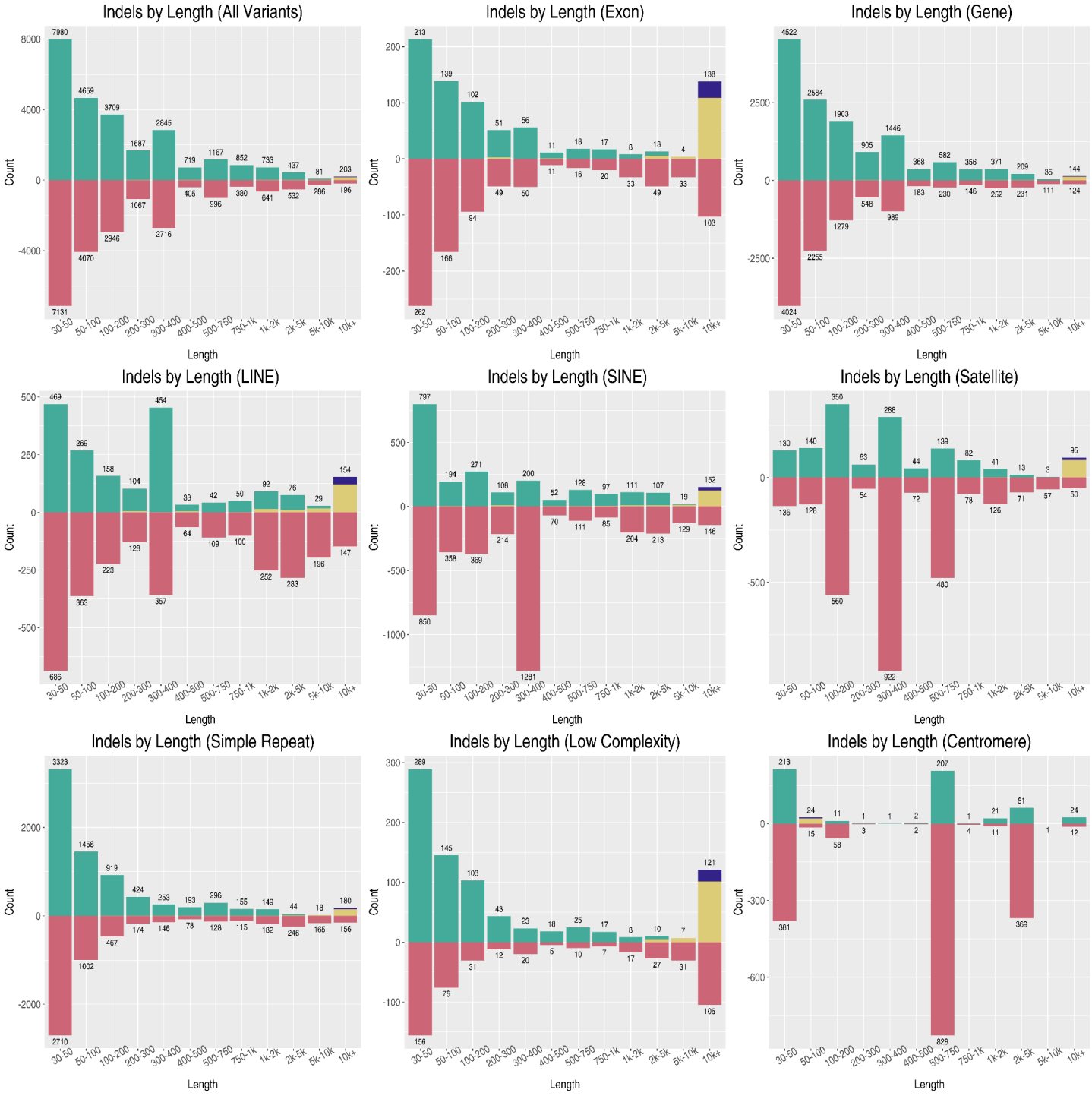

Supplementary Figure 30. Variant Type/Length Distribution in HG002 HiFi Trio by Genomic Context.

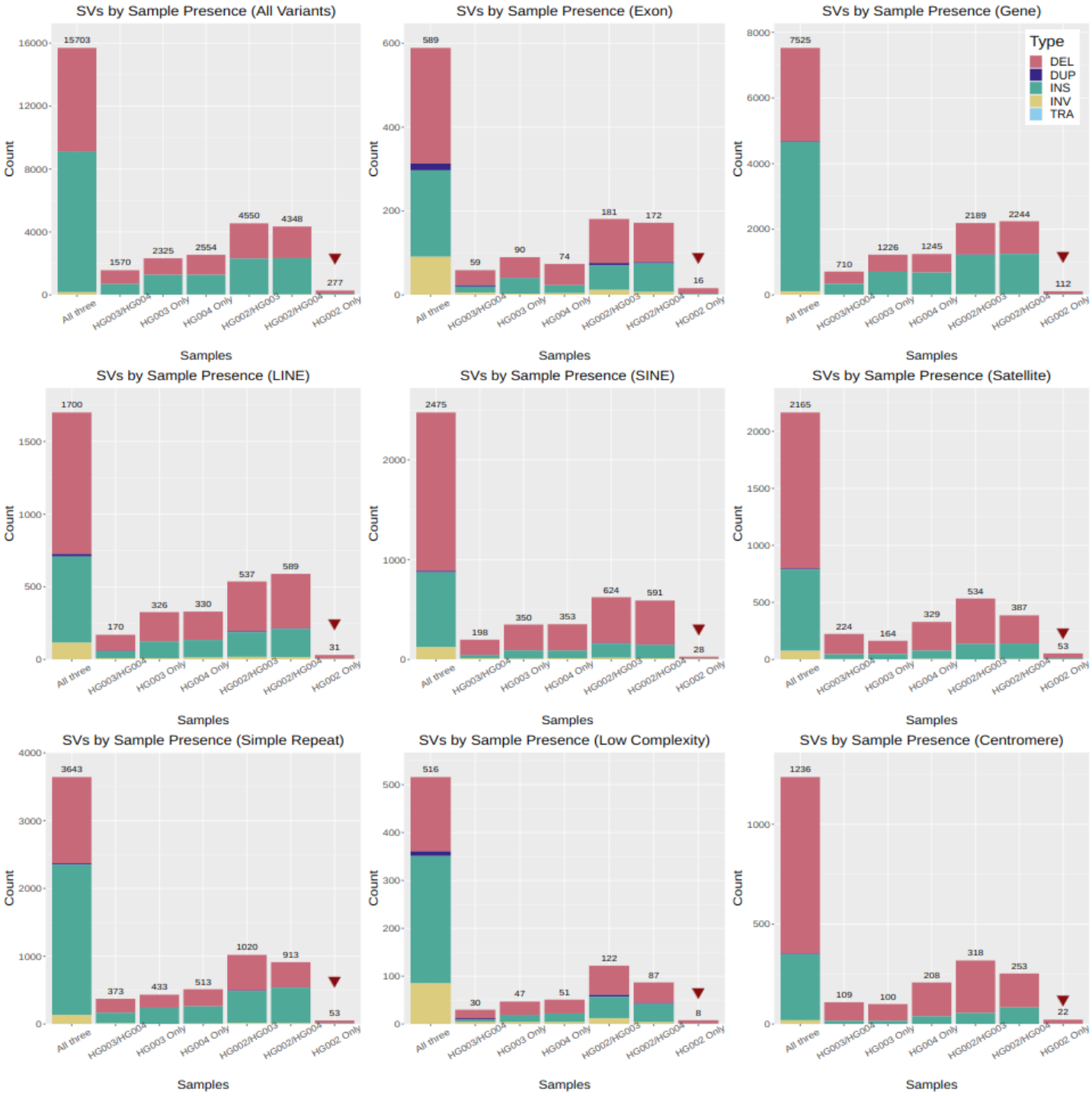

Supplementary Figure 31. HG002 HiFi Trio SV Sample Presence by Genomic Context.

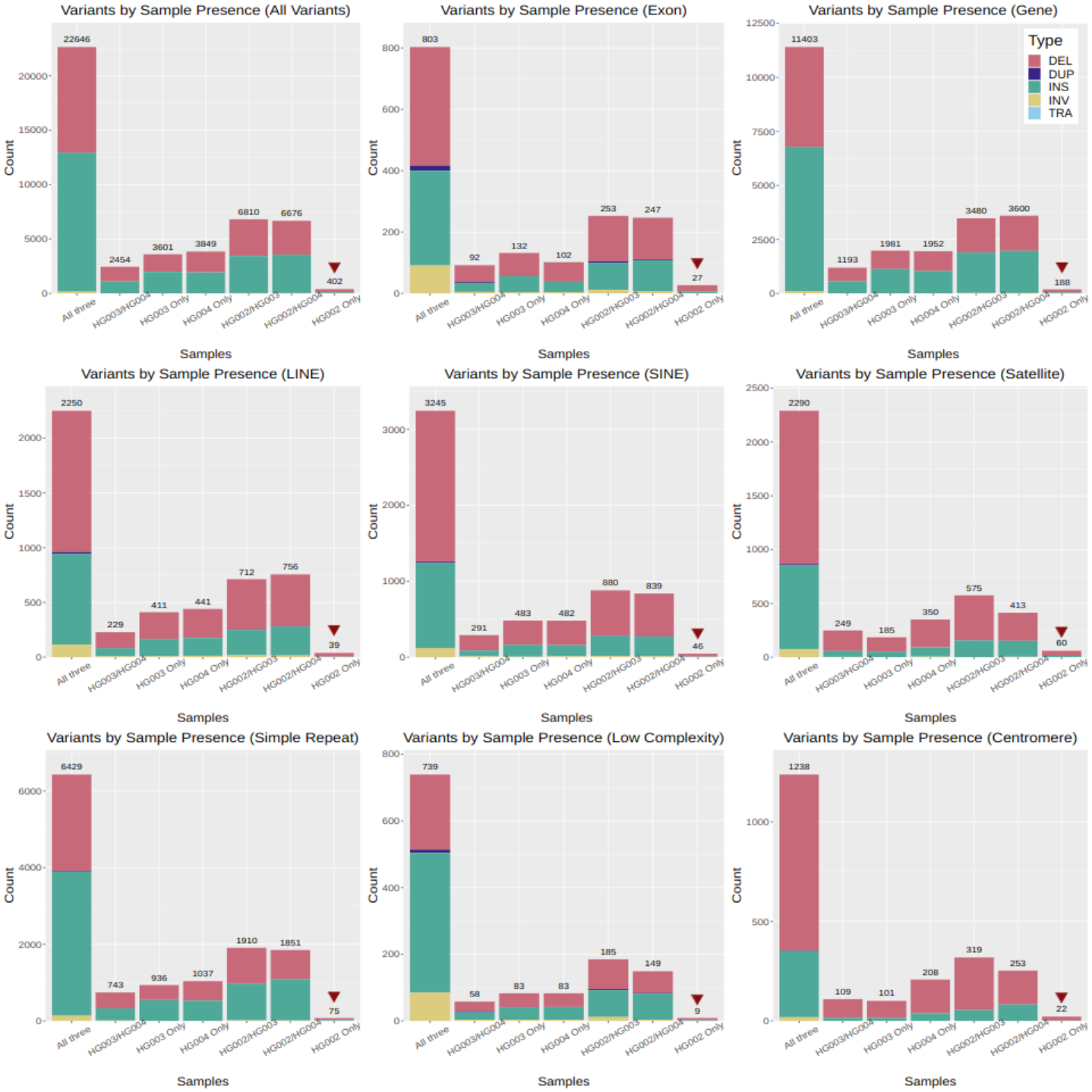

Supplementary Figure 32. HG002 HiFi Trio SV and Indel Sample Presence by Genomic Context.

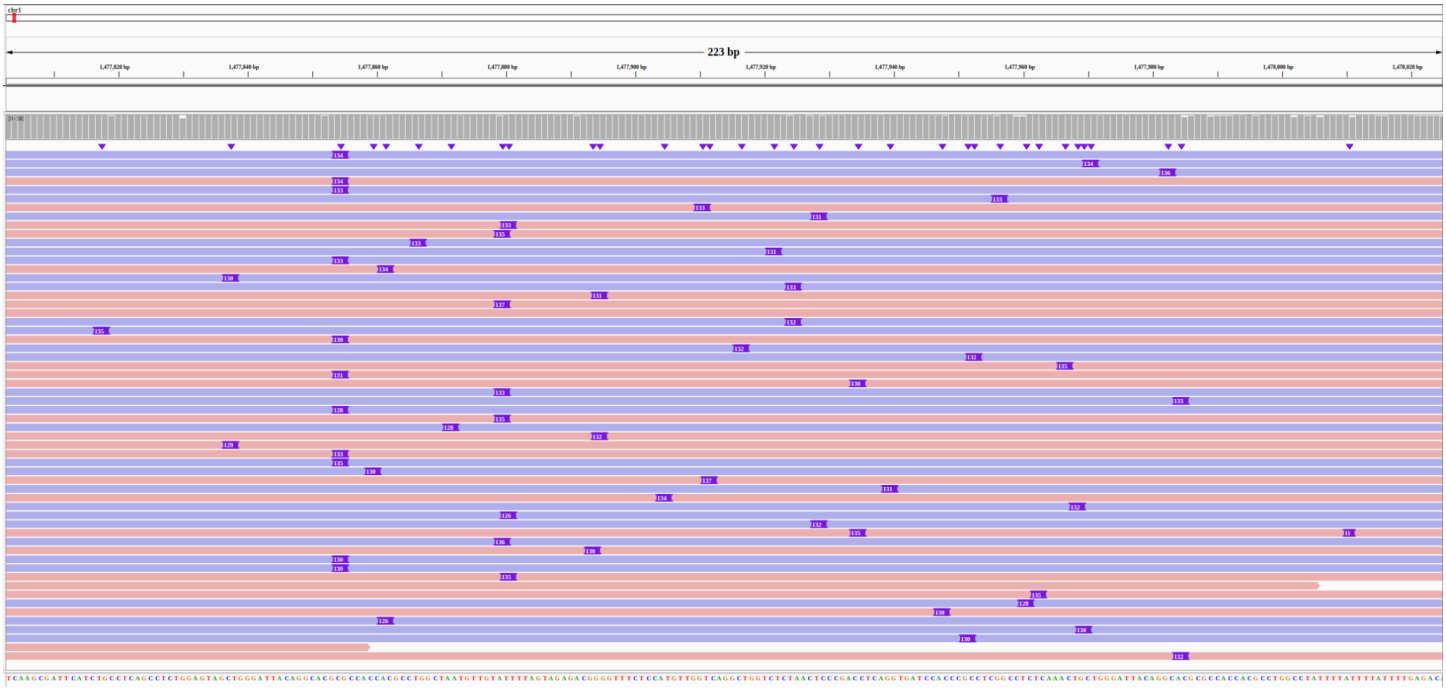

Supplementary Figure 33. Variable Breakpoints and Sequences among Individual Reads.
This figure shows an insertion SV in HG002 at chr1:1477881 in which the breakpoints and sequence length vary among individual ONT reads.

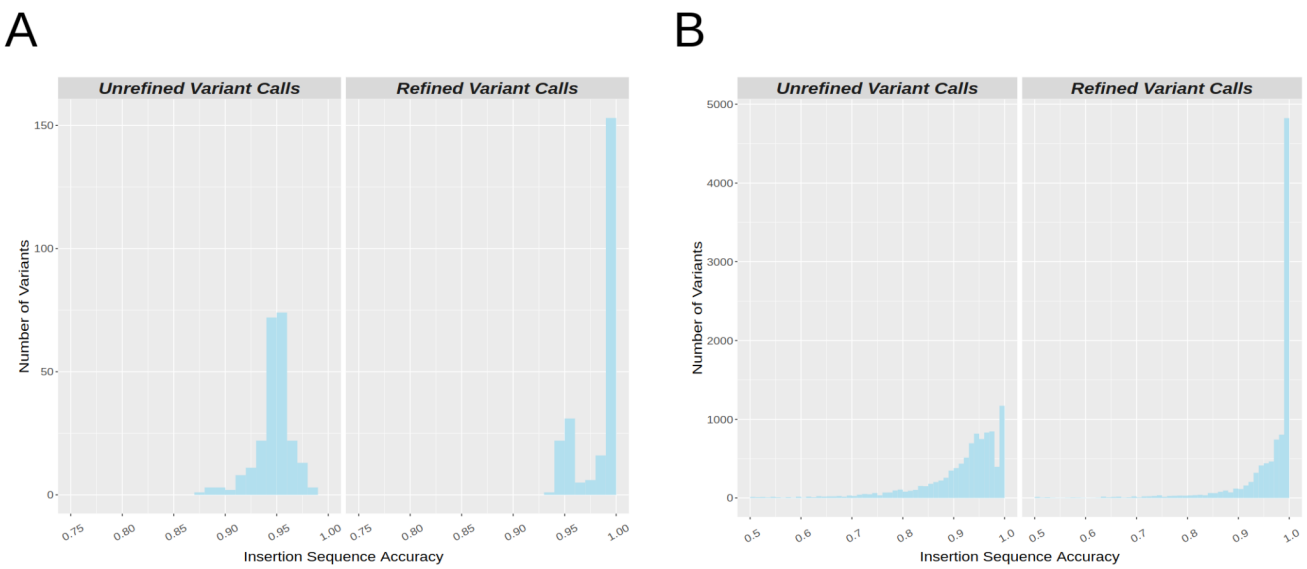

Supplementary Figure 34. Improved Insertion Sequence Accuracy with Iris.
a.) The distribution of insertion sequence accuracy in 200 SV calls from the simulation of human chromosome 1 with and without Iris refinement.
b.) The distribution of insertion sequence accuracy in the HG002 SV calls derived from ONT reads, using the HiFi calls as ground truth, with and without Iris refinement.

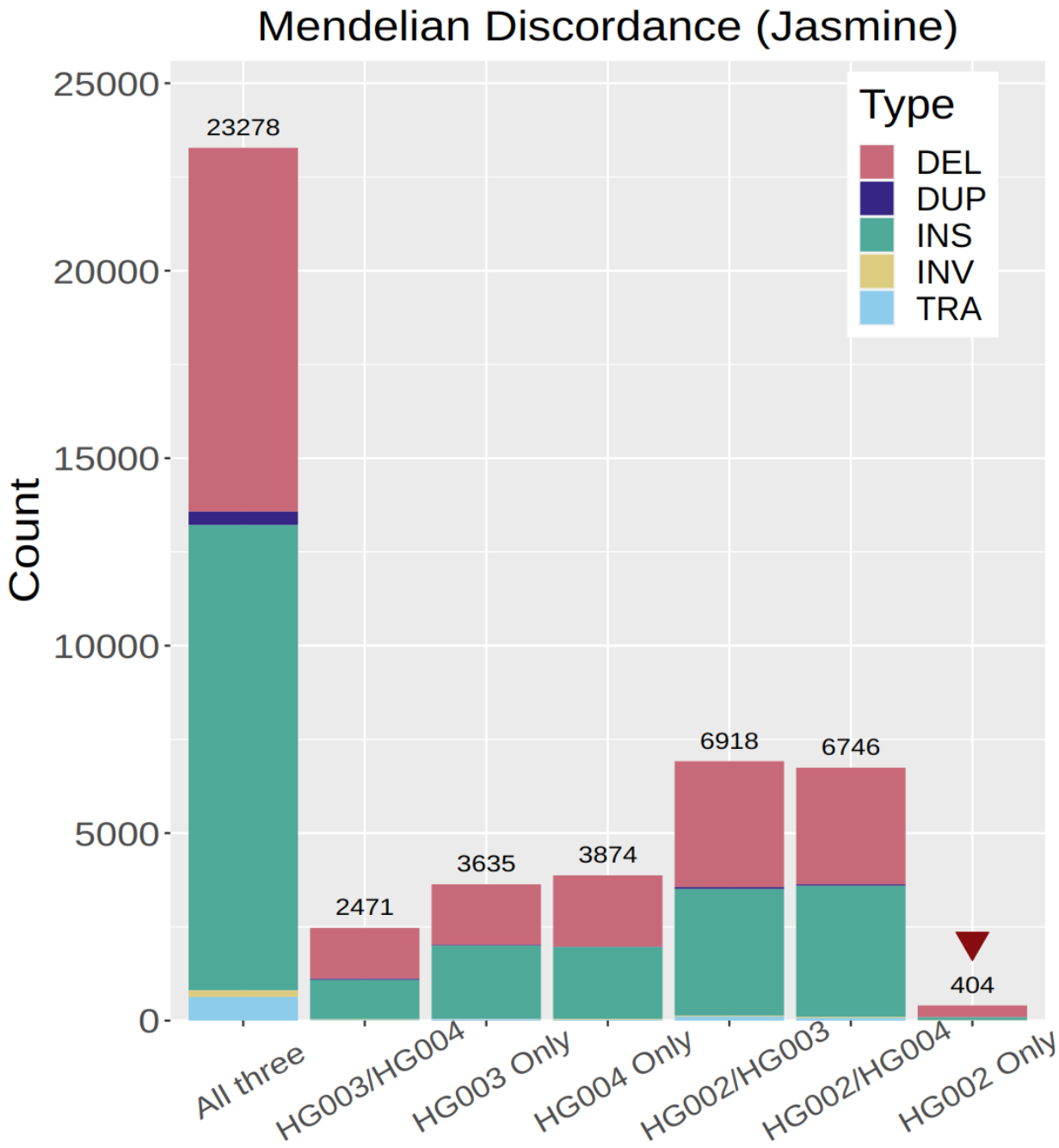

Supplementary Figure 35. Discordance in HG002 of Jasmine for SVs and Indels
The number of SVs and indels called in each subset of individuals when using our optimized pipeline to call variants from HiFi data in the HG002 trio.

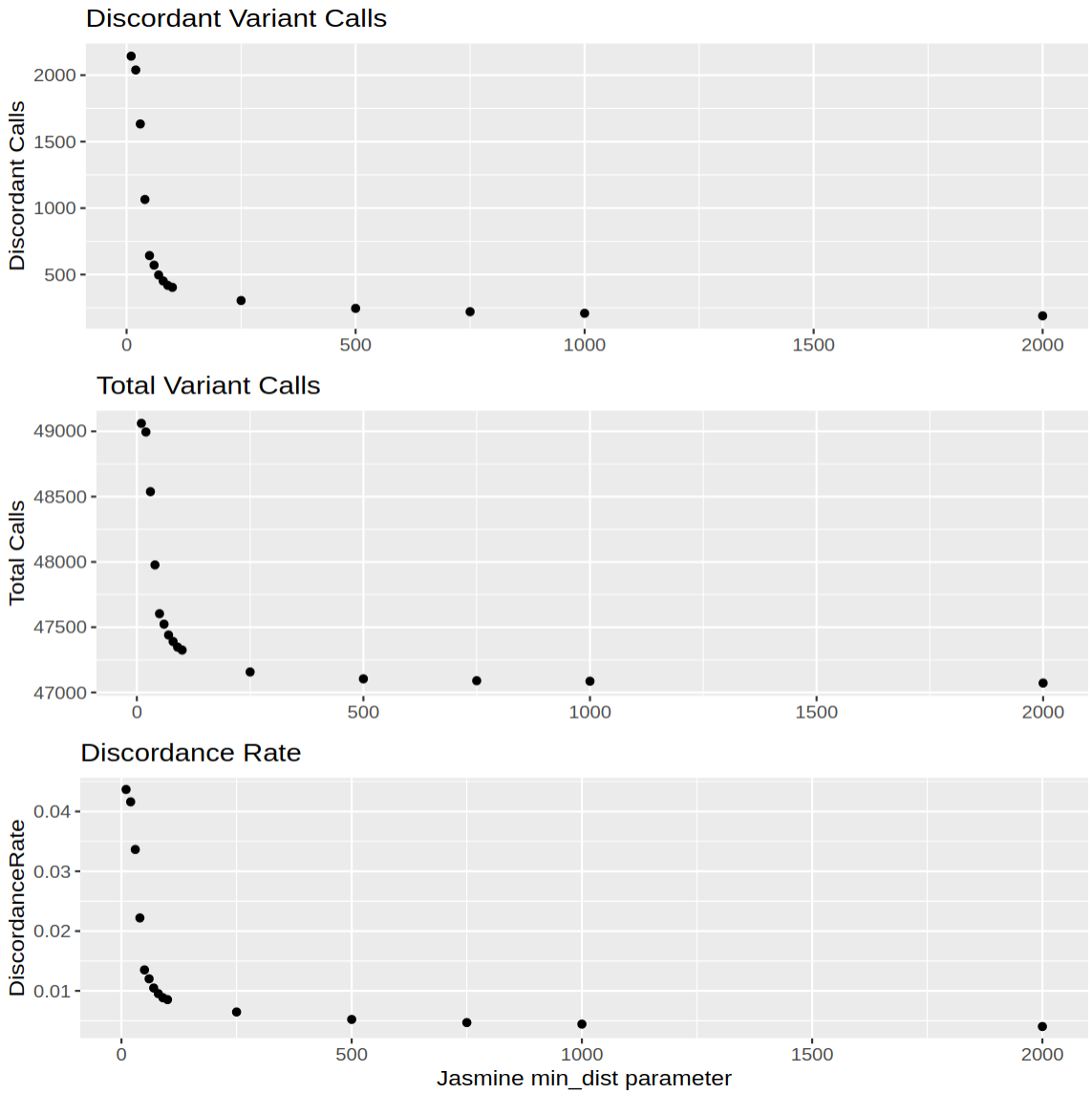

Supplementary Figure 36. Mendelian Discordance across Jasmine Distance Thresholds in the HG002 Trio.

We varied the *min_dist* parameter when merging SVs and indels in HG002, HG003, and HG004, and observed the total number of variants, the number of discordant variants, and the discordance rate for each run.

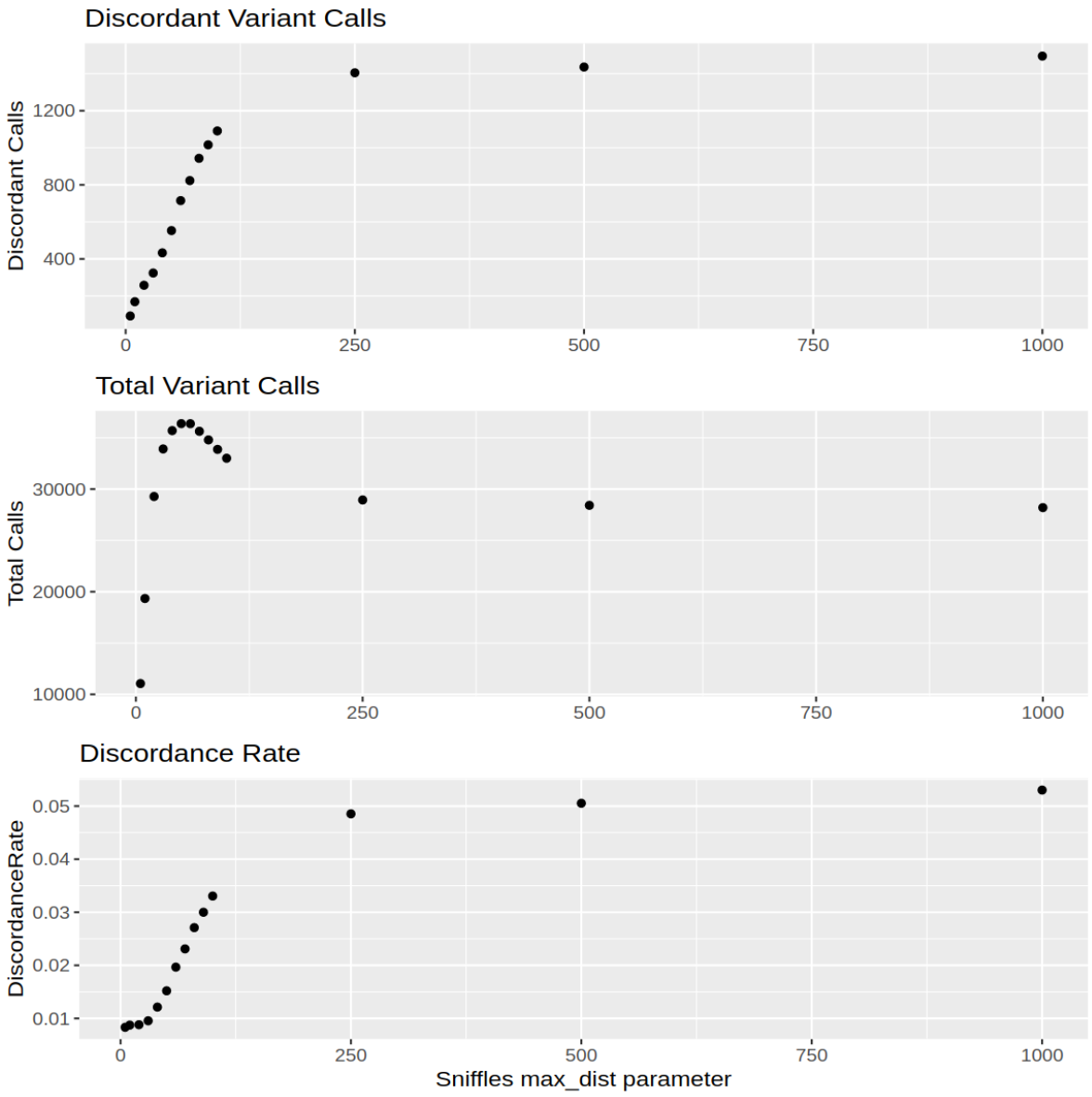

Supplementary Figure 37. Optimized Variant Calling Parameters for CLR.
We called SVs and indels in HG002, HG003, and HG004 from CLR reads using different values of the *max_dist* parameter in sniffles and merged each trio callset with Jasmine. For each *max_dist* value we measured the total number of variants in the trio, the number of discordant variants, and the discordance rate.

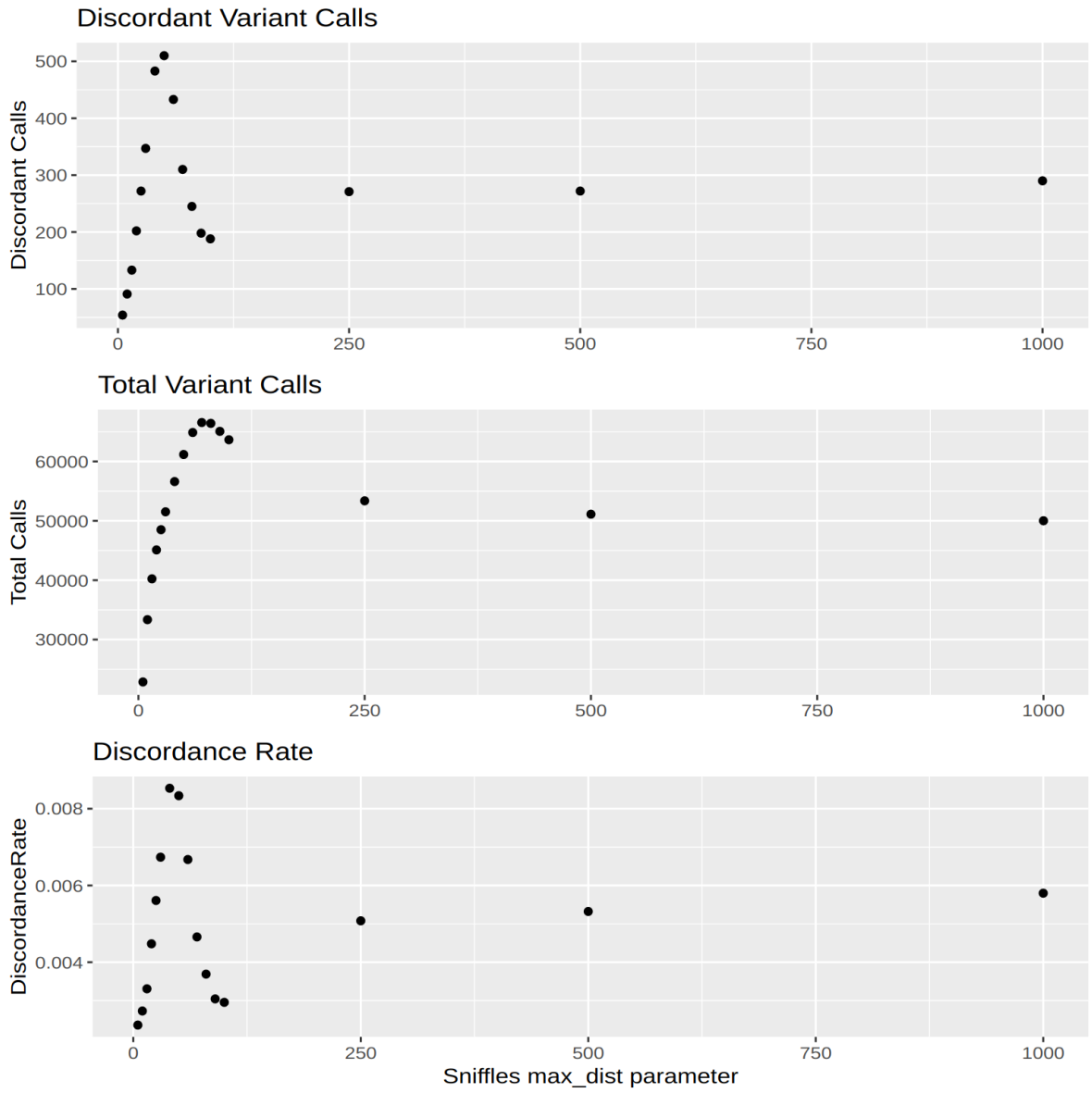

Supplementary Figure 38. Optimized Variant Calling Parameters for ONT.
We called SVs and indels in HG002, HG003, and HG004 from ONT reads using different values of the *max_dist* parameter in sniffles and merged each trio callset with Jasmine. For each *max_dist* value we measured the total number of variants in the trio, the number of discordant variants, and the discordance rate.

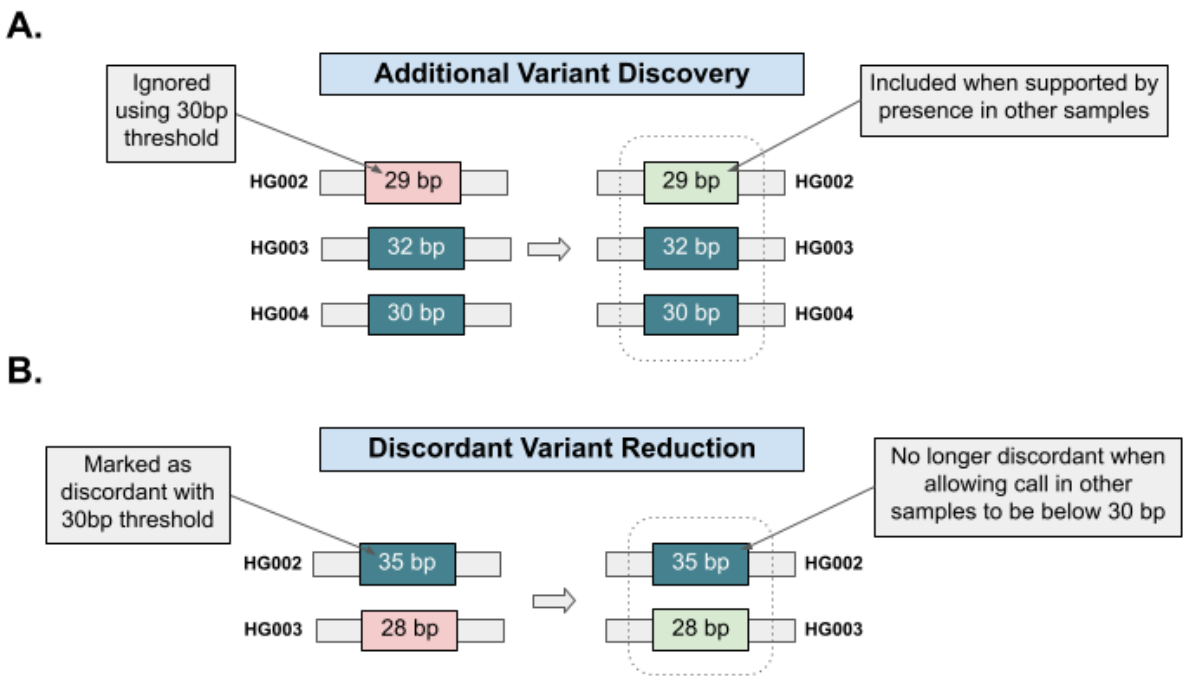

Supplementary Figure 39. Double Thresholding to Reduce Threshold Effects.
To avoid cases where variants with length or read support near the variant calling threshold are detected in some but not all samples where they are present, we use a double threshold. In the case of trio analysis, we are able to both **a.)** discover more variants in the child and **b.)** reduce the number of discordant variants compared to using a single threshold.

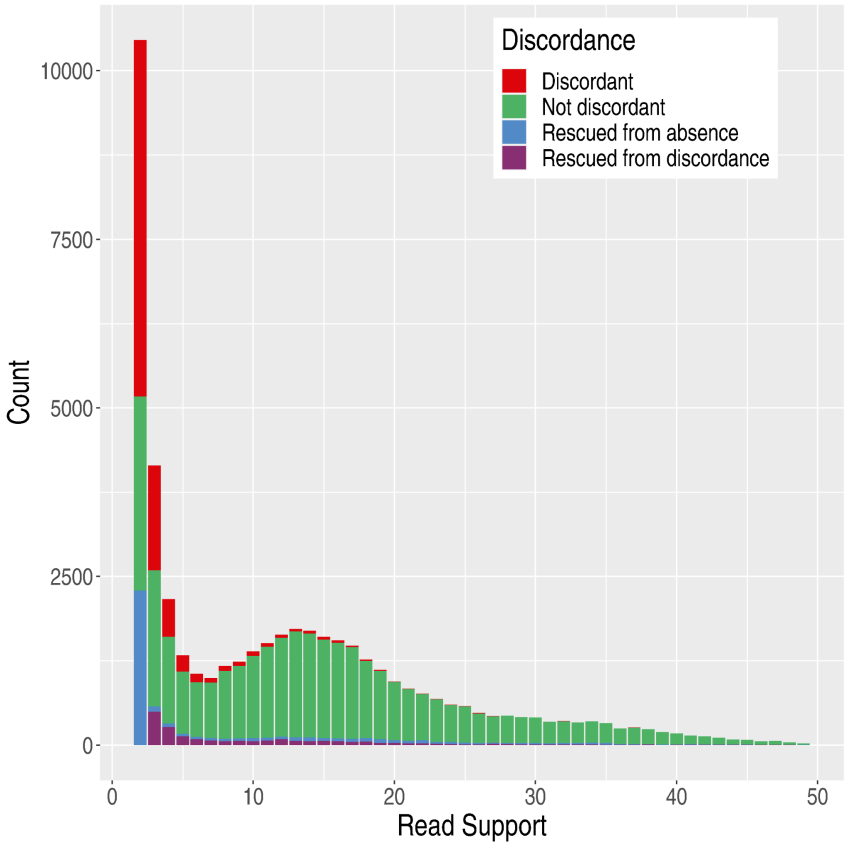

Supplementary Figure 40. Discordance by Read Support with Double Thresholding.
This illustrates the read support distribution of SVs and indels in HG002 called from HiFi data. SVs and indels were called with a more lenient length threshold of 20bp, but only those which were merged with a variant with length at least 30bp in a different sample were kept. “Rescued from absence” refers to variants which would have been missed in HG002 using a single threshold. “Rescued from discordance” refers to variants which would have been discordant in HG002 with a single threshold, but which we were able to detect in one or both parents with double thresholding. As the read support increases, the number of discordant variants decreases, but even among variants with low read support there are many which are not discordant, and double thresholding improves our ability to resolve them.

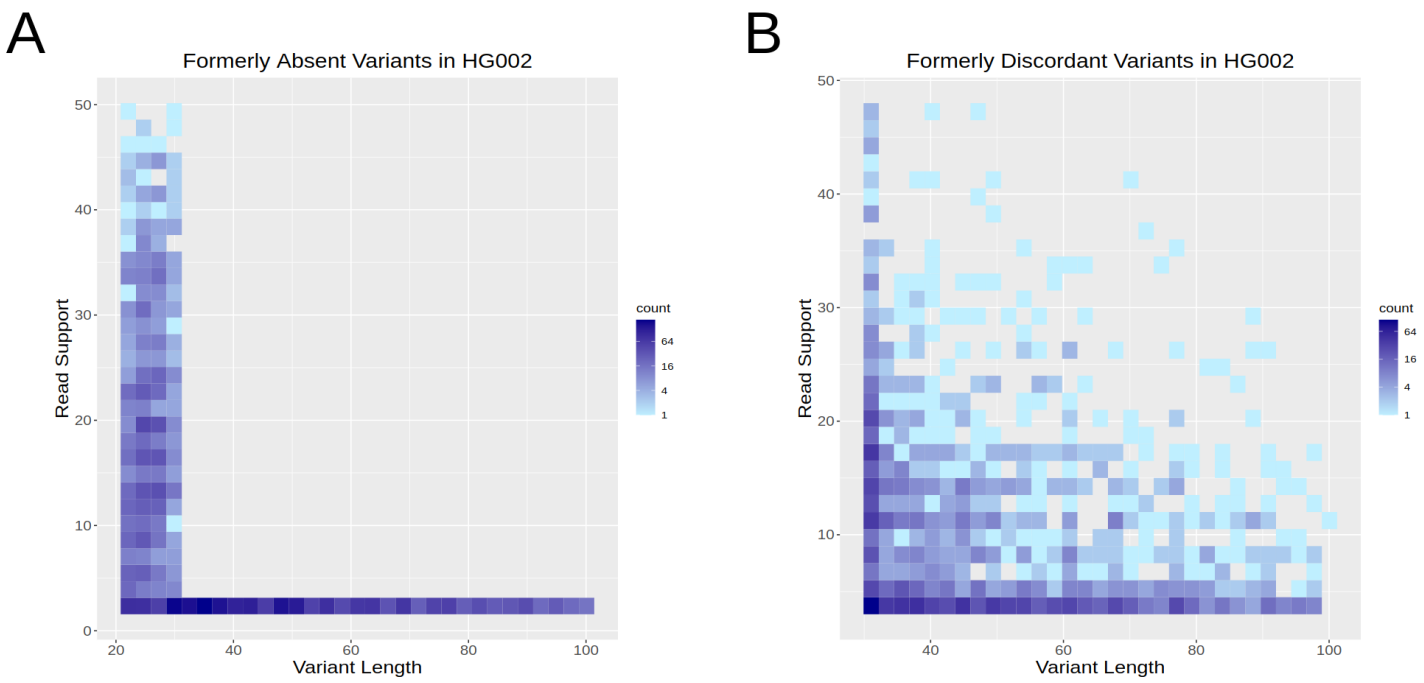

Supplementary Figure 41. Length and Read Support among HG002 HiFi Variants with Double Thresholding.

a.) The length and read support of variants which would have missed in HG002 if using only a single threshold.

b.) The length and read support of variants which would have been discordant in HG002 if using only a single threshold.

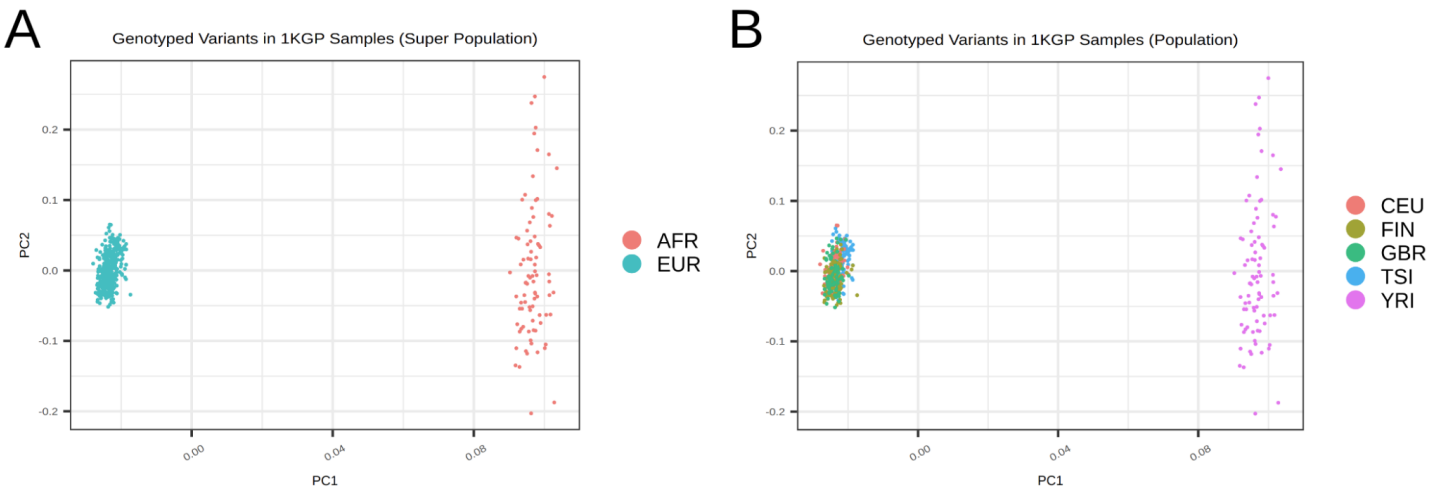

Supplementary Figure 42. PCA of 1KGP SV and Indel Genotypes.
A two-dimensional projection of the absence/presence vectors of all genotyped variants in the 444 samples from the 1000 Genomes Project that we used for eQTL analysis, colored by **a.)** superpopulation and **b.)** population.

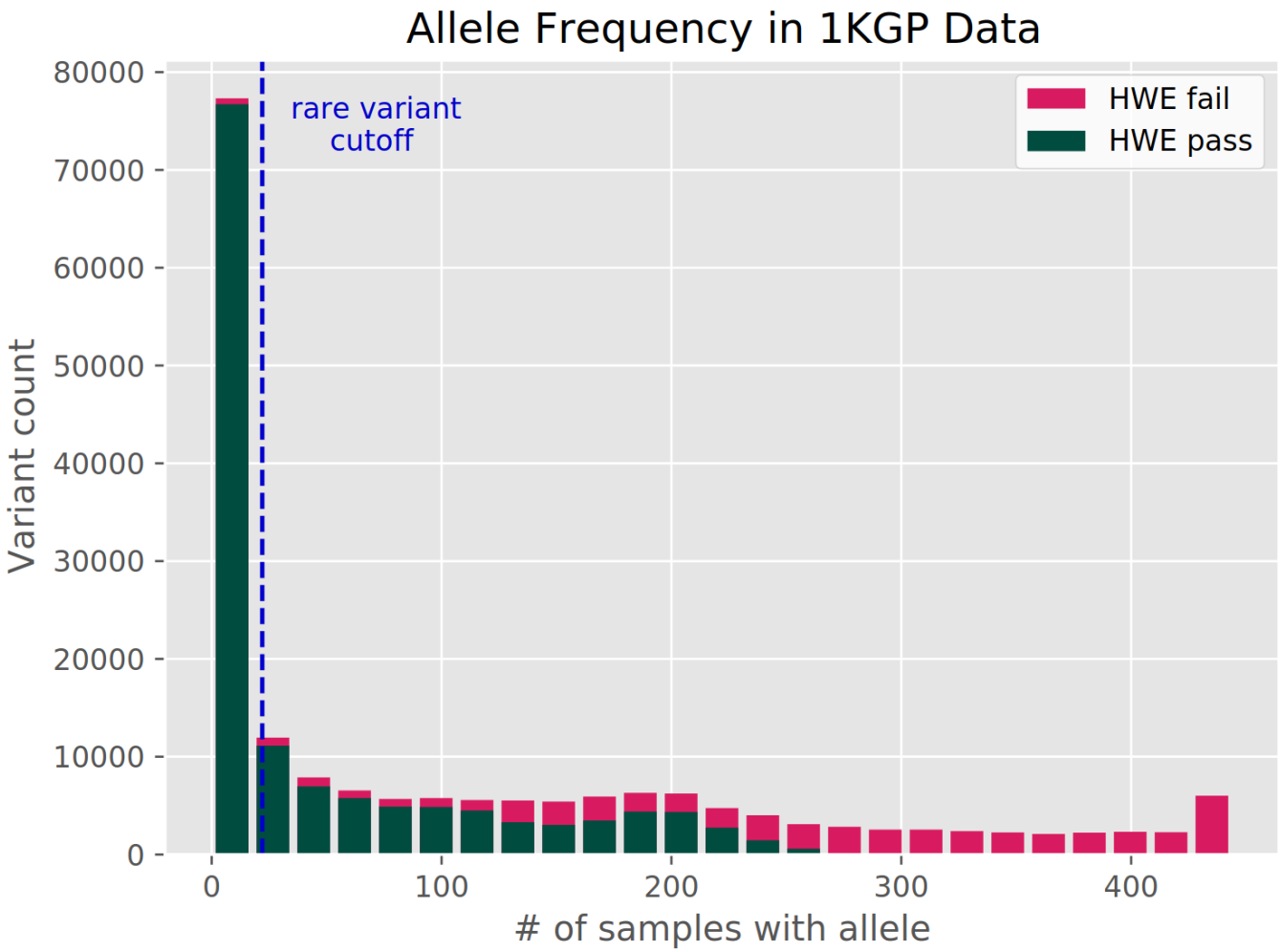

Supplementary Figure 43. 1KGP Allele Frequencies before and after HWE Filtering.
Histogram of variant allele frequencies passing and failing the HWE test to filter out variants genotyped by Paragraph in the 1000 Genomes samples that do not match expected Hardy-Weinberg allele frequencies, following best practices [43]. We later filter out rare variants with allele frequency less than 0.05 (dashed blue line).

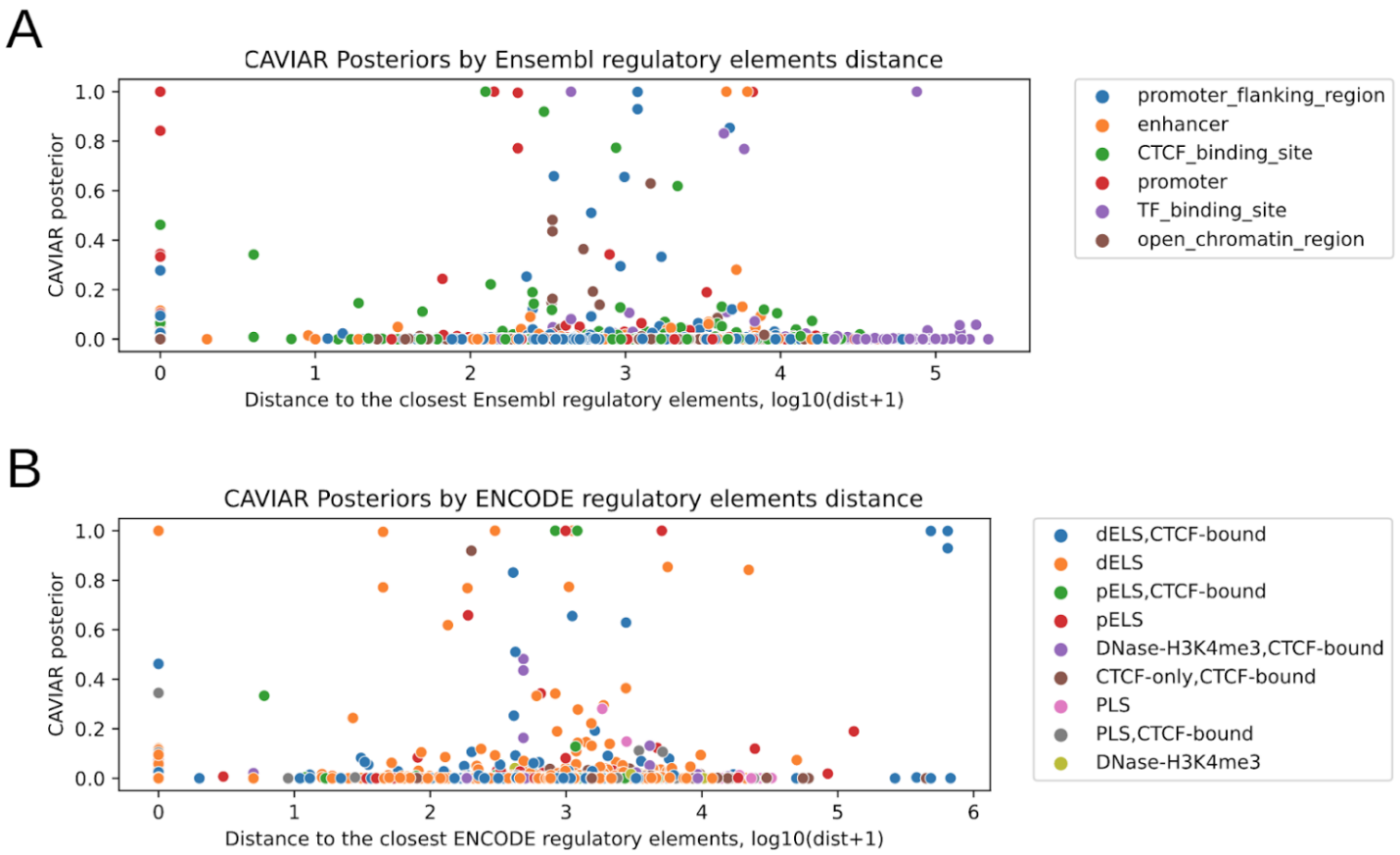

Supplementary Figure 44. 1KGP CAVIAR Score vs. Distance to Regulatory Elements.
Distances to nearest regulatory elements colored by the type of the nearest elements for SVs and indels genotyped with Jasmine in 1KGP samples. **a.)** Log-scaled distances of SVs and indels to various regulatory elements in Ensembl regulatory build. **b.)** Log-scaled distances of SVs and indels to the nearest regulatory elements in ENCODE cis regulatory regions. Both databases are independently derived and most of the variants with high CAVIAR posteriors are within the 6kb proximal region of regulatory elements. The types of elements near those high-posterior variants, are primarily promoters, enhancers which are relevant to the regulation of gene expression.

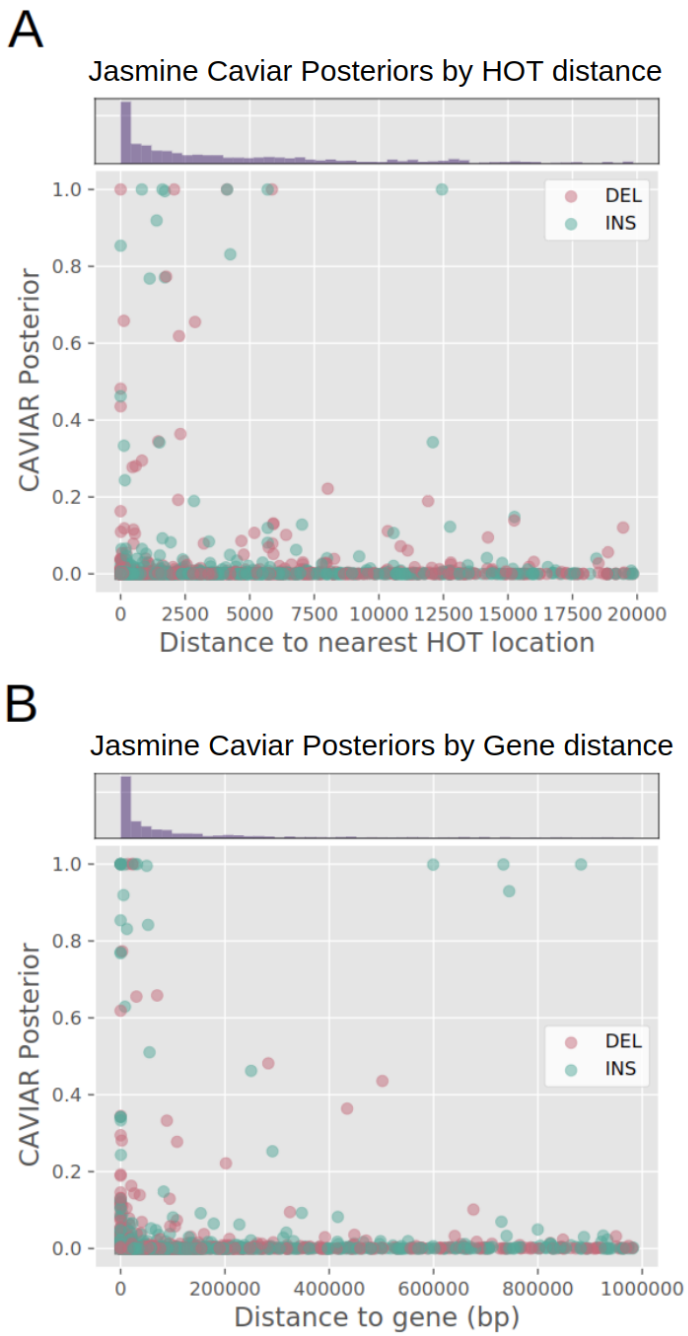

Supplementary Figure 45. 1KGP Jasmine Caviar Posteriors by HOT Region and Gene Distance. **a.)** Jasmine SV and indel (genotyped in 1KGP samples) distance to nearest HOT (Highly Occupied by Transcription factors) regions from FunSeq2. Histogram shows distribution of distances to HOT regions. **b.)** Jasmine SV and indel distance to nearest gene. Histogram shows distribution of distances to genes.

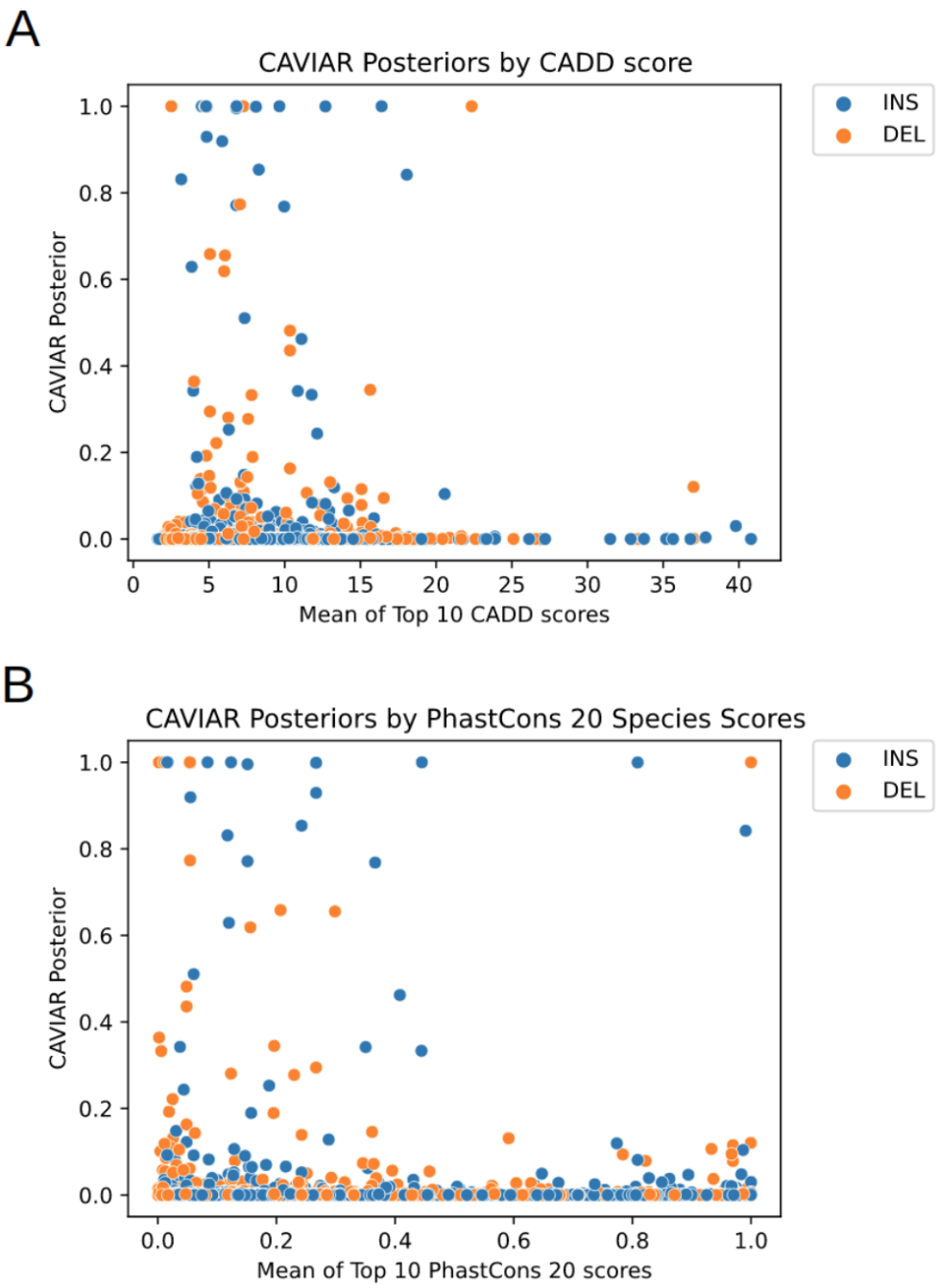

Supplementary Figure 46. 1KGP CAVIAR Score vs. CADD and PhastCons Scores.
The mean of the top 10 single-base **a.)** CADD scores scaled as positive Phred-like values and **b.)** PhastCons scores among 20 core mammalian species are calculated in each variant interval for SVs and indels genotyped by Jasmine in 1KGP samples. Higher CADD scores indicate higher pathogenic likelihood, while higher PhastCons scores indicate strongly conserved regions. We do not observe evidence of enrichment for conservedness or pathogenicity among variants with high CAVIAR posteriors.

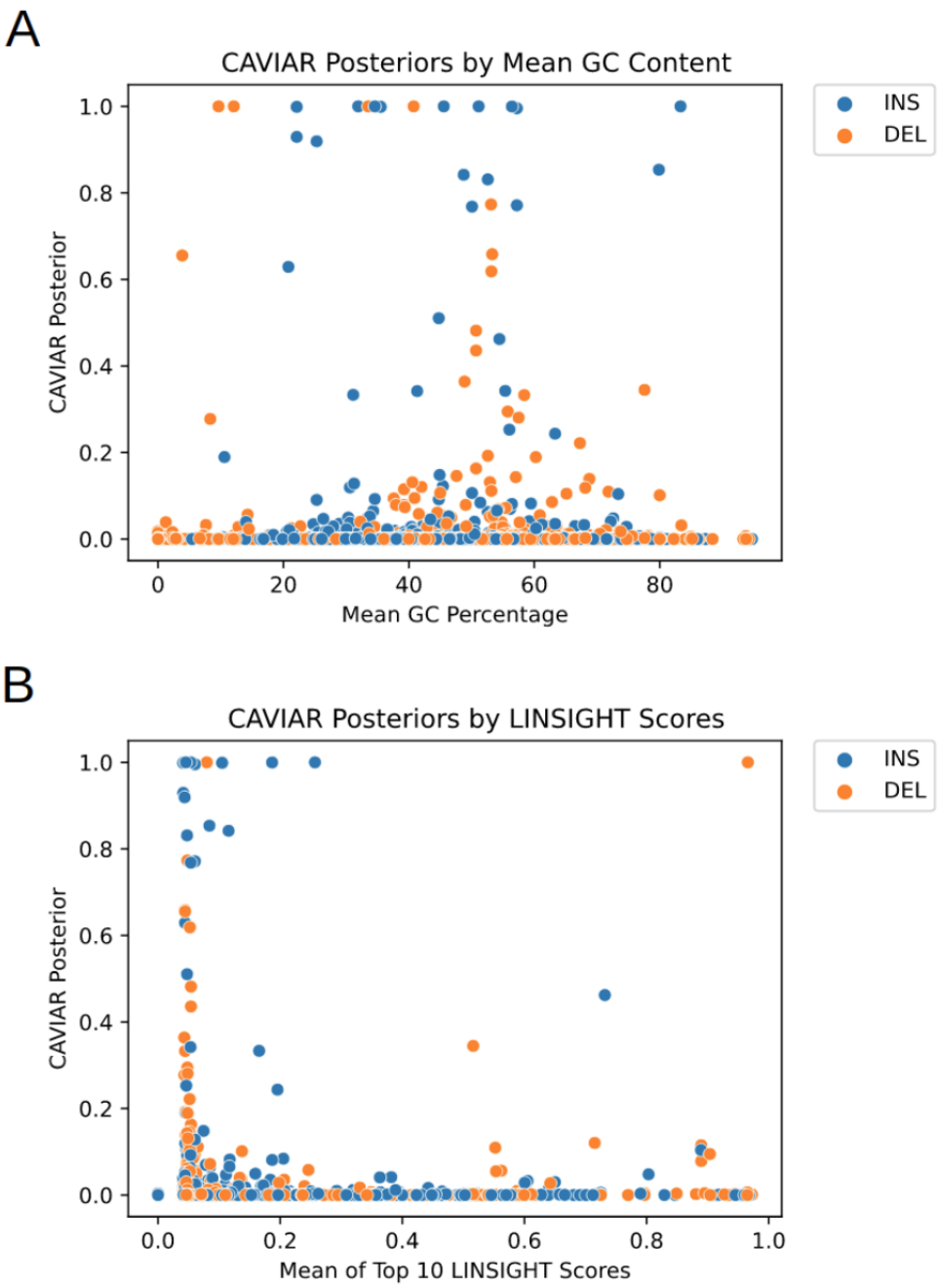

Supplementary Figure 47. 1KGP CAVIAR Score vs. GC Content and LINSIGHT Score.
a) The mean GC content and **b)** the mean of the top 10 single-base LINSIGHT scores are calculated for each variant interval for SVs and indels genotyped by Jasmine in 1KGP samples. GC content is measured as a percentage and is taken from the corresponding track of the UCSC Genome Browser. LINSIGHT scores represent posterior probabilities that each variant has non-coding consequences. We do not observe evidence for variants with high CAVIAR posteriors to be enriched for extreme GC content or high LINSIGHT scores.

Supplemental Note 1. Jasmine Merging Algorithm.

```
// Takes a set of variants and merges them
MergeAllVariants(vars)
{
    MergedSet = {}

    // Separately merge each chromosome and type
    for(chr in unique({v.chr | v ∈ vars})
    {
        for type in unique({v.type | v ∈ vars})
        {
            SetToMerge = {v | [(v ∈ vars) ∧ (v.chr = chr) ∧ (v.type = type)]}
            MergedSet = MergedSet ∪ MergeSingleGraph(SetToMerge)
        }
    }
    return MergedSet
}



// Merges a set of variants that have the same chromosome and type
MergeSingleGraph(vars)
{
    // Convert SVs to 2D points based on their positions and lengths
    for(v in vars)
    {
        x = v.pos
        y = v.length
        if(v.type == "TRA") y = v.pos2
        v.point2D = (x, y)
    }

    // Add all points to a KD Tree which supports rapid k-nearest neighbor queries
    kdtree = new KDTree()
    kdtree.addAllPoints({v.point2D | v ∈ vars)

    // Initialize a heap to store variant pairs to consider merging
    PairsToProcess = new MinHeap()

    for(v in vars)
    {
        // Initially all variants are in their own component
        v.ComponentId = v.id

        // Initially store the 4 nearest neighbors for each variant
        v.UpcomingNeighbors = kdtree.kNearestNeighbors(v.point2D, 4)

        // Keep track of how many neighbors of each SV have been considered so we know
        // when to refresh the list of upcoming neighbors
        v.NeighborsChecked = 0

        // Add the nearest neighbor for each point to the heap of pairs to consider
        // with the priority key being the Euclidean distance between them
        DistToNearest = EuclideanDistance(v.point2D,  v.UpcomingNeighbors[0])
        PairsToProcess.add(Pair(v, v.UpcomingNeighbors[0].id), DistToNearest)
    }

    // Iterate over the heap until we have no more pairs to consider
    while(PairsToProcess.size > 0)
    {
        NearestPair = PairsToProcess.getMin()

        first = NearestPair.first
        second = NearestPair.second

        // If their distance is bigger than the first point's threshold we can stop
        // considering any of the first point's neighbors since they will all be bigger
        if(NearestPair.dist > first.DistanceThreshold) continue

        CanMerge = true

        SamplesWithFirst = unique({v.Sample | v.ComponentID = first.Component})
        SamplesWithSecond = unique({v.Sample | v.ComponentID = second.Component})
```

```
        // If the SVs come from the same sample or have been merged with anything
        // from the same sample, this merge cannot occur
        if(SamplesWithFirst ∩ SamplesWithSecond ≠ ∅)
        {
            CanMerge = False
        }

        // If the distance is too large, the merge cannot occur
        if(NearestPair.dist > second.DistanceThreshold)
        {
            CanMerge - False
        }


        // Perform merging of this variant pair if the merge is valid
        if(CanMerge)
        {
            Merge(vars, first, second)
        }

        // Now get the next nearest neighbor for the first variant in the pair

        first.NeighborsChecked += 1

        // If we used everything we got from the KDTree query, make another
        // query for twice as many neighbors
        if(first.NeighborsChecked == first.UpcomingNeighbors.size)
        {
            NewSize = 2 * first.UpcomingNeighbors.size
            first.UpcomingNeighbors = kdtree.kNearestNeighbors(first.point2D, NewSize)
        }

        // Get the next neighbor from the list and add the pair to the heap
        NextNeighbor = first.UpcomingNeighbors[first.NeighborsChecked]
        DistToNext = EuclideanDistance(v.point2D,  NextNeighbor)
        PairsToProcess.add(Pair(v, NextNeighbor.id), DistToNext)
    }

    // Group variants by component and return
    Results = new Map()
    for(component in unique(vars.ComponentID))
    {
        Results[component] = {v | [(v ∈ vars) ⋀ (v.ComponentID = component)]}
    }

    return Results
}


// Merge a pair of variants together by iterating over the smaller component
// and updating their component IDs to match the other variants'.
Merge(vars, first, second)
{
    FirstComponent = {v | [(v ∈ vars) ⋀ (v.ComponentID = first.ComponentID)]}
    SecondComponent = {v | [(v ∈ vars) ⋀ (v.ComponentID = second.ComponentID)]}

    if(FirstComponent.size > SecondComponent.size)
    {
        for(v in SecondComponent)
        {
            v.ComponentID = first.ComponentID
        }
    }

    else
    {
        for(v in FirstComponent)
        {
            v.ComponentID = second.ComponentID
        }
    }

}
```

Supplemental Note 2. Commands Used.

Jasmine Merging

```
$ jasmine file_list=FILELIST out_file=MERGED_VCF max_dist_linear=0.5
min_dist=100
```

dbsvmerge Merging

```
$ dbSV_merge -f FILELIST -o MERGED_VCF -l 2.0 -r 0.4
```

svpop Merging

```
$ python $SVPOPPATH/merge.py FILELIST SAMPLE_LIST MERGED_VCF
```

SURVIVOR Merging

```
$ SURVIVOR merge FILELIST 1000 1 1 1 0 1 MERGED_VCF
```

svtools Merging

```
$ svtools lsort -r -f FILELIST OUTPUT_SORTED_VCF
$ svtools lmerge -i SORTED_VCF -f 250 > MERGED_VCF
```

svimmer Merging

```
$ python svimmer FILELIST CHROMOSOME_LIST --threads 2 --output MERGED_VCF
--max_distance 1000 --max_size_difference 1000 --ids
```

sv-merger Merging (separate for each chromosome and SV type)

```
$ python main.py FIND_TRR_OVERLAPS SINGLE_SAMPLE_SVS_TSV
trf_coords/chr1.trf.sorted.gor TR_OVERLAPS_FILE 5
$ python $BINDIR/main.py PRE_CLUSTER TR_OVERLAPS_FILE PRECLUSTERED_FILE 50 1
$ python $BINDIR/main.py FIND_CLIQUES PRECLUSTERED_FILE MERGED_TSV
TRR_MERGED_TSV DEL 85 50
```

Paragraph Genotyping

```
$ multigrmpy.py -m SAMPLE_MANIFEST -i POPULATION_SV_VCF -M [20*DEPTH] -o
OUTPUTFOLDER -r REFERENCE --threads 24 --scratch-dir SCRATCHFOLDER
```

More details of the preprocessing steps and commands used for different merging methods can be found here: https://github.com/mkirsche/SVMergingMethodComparison.

All code for eQTL analysis of SVs can be found here: https://github.com/gautam-prab/jasmine-sv-eqtls.